Transdermal Photopolymerization of Hydrogels for Tissue Engineering

By

Jennifer Hartt Elisseeff

B.S. Chemistry
Carnegie Mellon University, 1994

Submitted to the Division of Health Sciences and Technology
In Partial Fulfillment of the Requirements for the Degree of

DOCTOR OF PHILOSOPHY

in Medical Engineering

at the

Massachusetts Institute of Technology
May, 1999
June 1999

Signature of Author_____
Division of Health Sciences and Technology
May 10, 1999

Certified by_____
Professor Robert Langer
Thesis Supervisor

Accepted by_____
Martha Gray, PhD.
J.W. Kieckhefer Associate Professor of Electrical Engineering
Co-Director, Division of Health Sciences and Technology

Transdermal Photopolymerization of Hydrogels for Tissue Engineering

By
Jennifer Hartt Elisseeff

Submitted to the Department of Health Sciences and Technology on May 10, 1999
In partial fulfillment of the requirements for the Degree of
Doctor of Philosophy in Biomedical Engineering

Photopolymerizations are widely used in medicine to create polymer networks for use in applications such as bone restorations and coatings for artificial implants. These photopolymerizations occur by directly exposing materials to light in "open" environments such as the oral cavity or during invasive procedures such as surgery. It hypothesized that light, which penetrates tissue, could cause a photopolymerization indirectly. Liquid materials could then be injected subcutaneously and solidified by exposing the exterior surface of the skin to light. To test this hypothesis, the penetration of UVA and visible light through swine and human skin fat and muscle was studied. Kinetic modeling was used along with the light transmission data to predict the feasibility of transtissue photopolymerization. To establish the validity of these modeling studies, transdermal photopolymerization was applied to tissue engineering using "injectable" cartilage as a model system. The ability to encapsulate chondrocytes was first studied *in vitro* using poly(ethylene oxide)-dimethacrylate and poly(ethylene glycol). Biochemical, histological and mechanical data demonstrated the formation of cartilage-like tissue. Subsequently, polymer/chondrocyte constructs were injected subcutaneously and transdermally photopolymerized. Implants harvested at 2, 4 and 7 weeks demonstrated collagen and proteoglycan production and histology with tissue structure comparable to native neocartilage. Finally, growth factors were incorporated into the photopolymerizing hydrogel system in a controlled-release system using poly(lactic-*co*-glycolic) acid microspheres. Insulin-like growth factor (IGF-1) and transforming growth factor (TGF-b) were encapsulated with chondrocytes *in vitro* and produced significant increases in proteoglycan and cell content. With further study, transdermal photopolymerization could potentially be used to create a variety of new, minimally invasive surgical procedures in applications ranging from plastic and orthopedic surgery to tissue engineering and drug delivery.

Thesis Supervisor: Robert Langer
Germeshausen Professor of Chemical and Biomedical Engineering

ACKNOWLEDGEMENTS

I would like to first thank Bob for the chance to work in the lab and for all of the guidance and exciting opportunities he has given to me. There are many people in the lab that has had a large and positive impact on my time in the lab. Special thanks go to Kristi Anseth for all of her help and friendship. I had a great time working with Kristi and look forward future endeavors, both professional and personal. Gordana has given me great guidance and wise advice (and let me work in a clean lab). Sachiko and Karen have been the best of friends throughout my time here and my life here would not have been the same without them. Dave Putnam, Keith Gooch and Torsten Blunk also provided much appreciated assistance. Winnette McIntosh, a UROP, diligently worked on a variety of assays and was a great person all around. Michele deMarco, another UROP, has also worked hard and will hopefully continue.

I have worked with many collaborators at Childrens and Mass General Hospitals to whom I would like to express gratitude. Mark Randolph and surgical fellows (Simone Ashiku, Derek Sims, Ron Silverman) in his lab have played a critical role in this project. Many thanks and I hope that successful continuation of our work will be possible. I would also like to express gratitude to Dr. Jay Vacanti and fellows in his lab (Clemente Ibarra, Tessa Hadlock) for all of their help. Nik Kolias and Bob Gilles from the Wellman labs for photomedicine at MGH also provided invaluable help with the tissue penetration experiments and great discussions.

I would like to thank Advanced Tissue Sciences for their funding. Anthony Ratcliffe gave me a lot of great advice and giudance and helped with a lot of ideas and experiments. I had a great time working with Suzie Riley (who helped with some

experiments) and Linette Edison. I also had some great discussions with Sharon Stevenson.

I would like to thank Pam Brown and Connie Beal for all of their support. Without them I wouldn't have gotten anything ordered, mailed, paid, etc.

Most importantly, I acknowledge my husband, Pierre, for his immense love and support (and help sessions on statistics and general mathematical issues) - and Sophie, for teaching me about life.

To Pierre and Sophie

TABLE OF CONTENTS page

LIST OF FIGURES

page

LIST OF TABLES

page

Chapter 1. Introduction

Medicine has moved toward minimally invasive procedures. Minimally invasive procedures generally cost less, and more importantly have reduced patient morbidity. This applies especially to the area of orthopedics. Joint related morbidity is a significant problem in the general population. Over one million Americans are treated for cartilage replacement.[1] It is estimated that 34 million Americans suffer from arthritis.[2] Younger patients, in particular athletes, also suffer from cartilage destruction from trauma. Previously researchers were interested in articular cartilage replacement using artificial prostheses. Current research is focused on joint surface regeneration using techniques including cartilage tissue engineering.

This thesis is concerned with development of a minimally invasive technique for hydrogel implantation. While techniques for minimally invasive implantation have a multitude of biomedical applications, this thesis examined applications in cartilage tissue engineering.

Hypothesis

Photopolymerization has been extensively studied for a variety of applications including dental implants.[3] Lasers and other light sources have gained popularity in medicine in a variety of applications including phototherapy treatments. Phototherapy treatments utilize light that penetrates the skin to stimulate photosensitive therapeutics.[4] The hypothesis for this thesis was that enough light would penetrate the skin or other tissues to cause a photopolymerization *in situ,* through tissues. For example, a prepolymer solution would be injected beneath the skin. The overlying skin would then be exposed to light that would penetrate the skin to cause a polymerization, avoiding the

need for an incision. This technique, transdermal photopolymerization, would thus provide a method to implant hydrogels in a minimally invasive manner.

Hydrogels have a high water content, porosity and mechanical integrity similar to natural biological tissues and matrix, making them an ideal candidate for tissue engineering applications.[5] Furthermore, growth factors incorporated into the hydrogel may potentially help to mimic natural extracellular matrix. It was hypothesized that a combination of a polymerizing polymer and nonphotopolymerizing polymer, combined to form a semi-interpenetrating network (semiIPN), would provide a matrix for cartilage development. The nonpolymerizing polymer is physically entrapped within the polymerizing polymer. Poly(ethylene oxide) (PEO) was chosen as a model polymer system with PEO-dimethacrylate (PEODM) as the photopolymerizing polymer with entrapped PEO. In addition, the semiIPN would provide a two-fold degradation system, with PEO quickly diffusing away to provide room for growing cells and the covalently connected PEODM remaining to provide implant structural integrity.

Specific Goals of the Thesis

1. Examine the potential for hydrogel implantation using transdermal photopolymerization through *in vitro* analysis of light and various tissue samples. Cell toxicity and photopolymerization kinetics will also be studied.

2. Analyze tissue forming potential of *in vitro* and *in vivo* encapsulation of chondrocytes in photopolymerizing hydrogel.

3. Incorporate growth factors in the photopolymerizing hydrogel in a controlled fashion to ameliorate tissue formation.

Outline of Thesis Contents

A general introduction to photopolymerization and light in medicine is provided in Chapter 2. The development of transdermal photopolymerization, toxicity analysis and photopolymerization kinetics is described in Chapter 2. *In vitro* photoencapsulation of chondrocytes was examined in Chapter 3, with both biochemical and mechanical analysis. Chapter 4 applies transdermal photopolymerization and chondrocyte encapsulation *in vivo*, examining tissue formation in athymic mice. Encapsulation of cartilage growth factors in PLGA microspheres and their use with photoencapsulated chondrocytes in the hydrogel are described in Chapter 5. Chapter 6 provides conclusions, potential implications and prospective future studies.

1. Langer, R. & Vacanti, J., Tissue Engineering. *Science* **260**, 920-926 (1993).
2. American Academy of Orthopedic Surgeons .
3. Decker, C., UV-Curing Chemistry: Past, Present and Future. *Journal of Coatings Technology* **59**, 97-106 (1987).
4. Kochevar, I., Photobiology. *Dermatological Clinics* **4**, 171-179 (1986).
5. Peppas, N. Hydrogels in Medicine and Pharmacy, Vol. II CRC Press, Boca Raton, FL, 1987.

Chapter 2: Transdermal photopolymerization for Minimally Invasive Implantation of Hydrogels*

2.1 Introduction

This chapter explores the use of transdermal photopolymerization as a method to implant biomaterials in a minimally invasive manner using light that penetrates skin and other tissues. The efficacy, toxicity and potential applications of transdermal photopolymerization are examined. A general introduction to photopolymerizations and the use of light in medicine is provided.

2.2 Background

2.2.1 *In situ* Photopolymerization. Fabricating polymers *in situ* provides many advantages for a variety of biomedical applications. For example, pre-polymerized liquid solutions or moldable putties can be easily placed in complex shapes (e.g., tooth caries) and subsequently reacted to form a polymer of exactly the required dimensions (see Section 2.2.3). Little, if any, additional shaping or modification of the implant is required. The adhesion of the polymer to surrounding tissue is generally significantly improved because of intimate contact of the polymer with the tissue during formation and the mechanical interlocking that can result from surface microroughness. In addition to these advantages, however, *in situ* polymerization also introduces many new challenges. Polymerization conditions for *in vivo* applications are quite adverse, including a narrow range of physiologically acceptable temperatures, requirement for nontoxic monomers

* This chapter was published in part in *Proceedings of the National Academy of Sciences*, 96:3104, 1999.

and/or solvents, moist and oxygen-rich environments, the need for rapid processing and clinically suitable rates of polymerization. However, photopolymerizations can overcome many of these limitations. A photopolymerization occurs when a photoinitiator and polymer (with groups sensitive to the initiating species) are exposed to a light source specific to the photoinitiator species. In some cases the photoinitiator may be attached to the polymer itself. Initiation of a photopolymerization does not require elevated temperatures, and the polymerization process is typically rapid (a few seconds to a couple of minutes), which allows the system to overcome oxygen inhibition and moisture effects present *in vivo* (see Section 2.4.2).

The concept of using light to polymerize or cure materials *in vivo* has been practiced in accessible places such as the oral cavity in dentistry, during invasive surgery, and more recently through minimally invasive surgery, leading to potentially new methods to prevent restenosis after angioplasty and post-surgical adhesions.[1-4] The above approaches require *directly* shining light on polymers to cause a photopolymerization, either as an open or invasive procedure. We hypothesized that enough light might traverse tissue, including skin, to cause a photopolymerization *transdermally,* and therefore provide a new method to implant biomaterials. Liquid biomaterials could be delivered subcutaneously through a small diameter needle, and would be converted from a liquid to a solid after only minutes of skin exposure to light (Figure 2.1). Transdermal photopolymerization could effectively allow implantation of biomaterials for plastic surgery applications, including both biodegradable and nondegrading polymers, and would potentially enable cells or drugs to be injected and encapsulated for tissue engineering, drug delivery or other applications. To test the

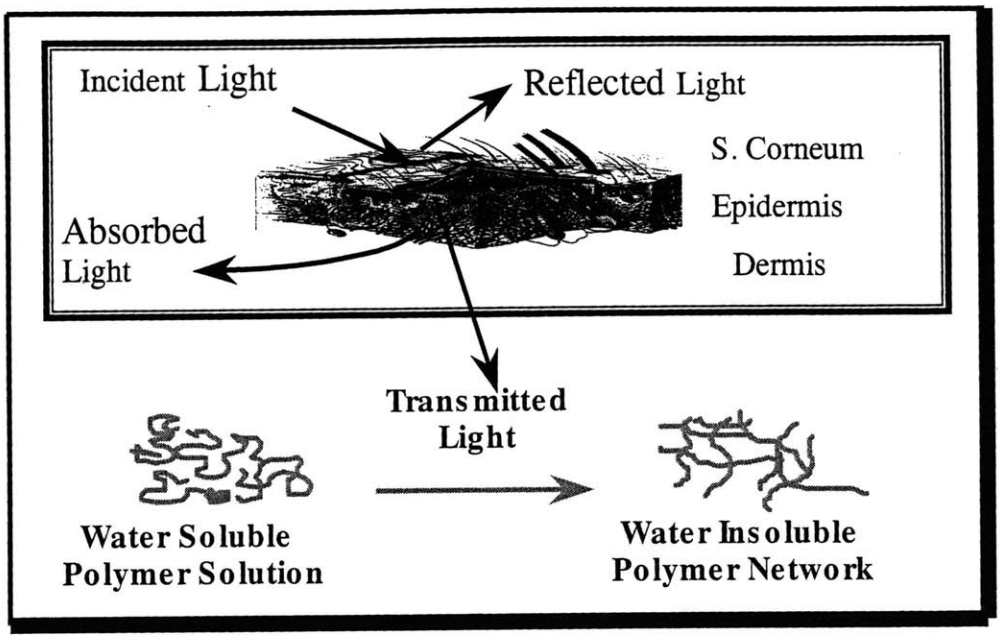

Figure 2.1. Schematic of transdermal photopolymerization demonstrating the interactions of light with skin and photopolymerization.

- **Physical Crosslinking**

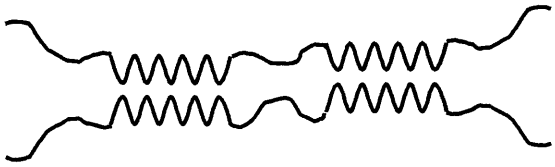

- **Ionic Crosslinking**

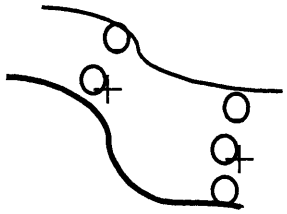

- **Covalent Crosslinking**

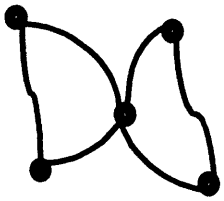

Figure 2.2. Methods of forming hydrogels: electronic, ionic or covalent interactions.

concept of transdermal polymerization, a model polymer hydrogel system using poly(ethylene oxide), PEO, was studied.

Hydrogels are candidate materials for many biomedical applications, including tissue engineering and drug delivery because of their high water content, transport properties, and tissue-like physical and mechanical behavior.[5] Hydrogels are comprised of polymer chains that are interconnected. The polymers may be connected through electronic (e.g. hydrophobic) interactions, ionic interactions or covalent interactions as depicted in Figure 2.2.

2.2.2 Light in Medicine. Light has made a significant impact in medicine and the progression to minimally and non-invasive therapies. Clinical use of laser technology has progressed with the development of small, inexpensive, and highly maneuverable lasers. Light has replaced the scalpel in a variety of surgeries, including ear nose and throat procedures, opthamology and plastic surgery. Thermal laser therapy (far infrared carbon dioxide and near infrared lasers) are used for removing large tumors.[6] Carbon dioxide lasers may be used to destroy tumors in inaccessible areas such as the brain. High precision eximer lasers are used for delicate surgeries to reshape the cornea. Near infrared lasers introduced endoscopically are used for palliative tumor debulking in the upper and lower gastrointestinal tract and large airways.[7] In addition, treatment of solid organ tumors has been examined. Using advanced imaging techniques (MRI, ultrasound and CT), lasers can be carefully guided to ablate solid organ tumors.[8] Solid tumors treated using laser treament include hepatic metastasis, breast cancer and prostatic hypertrophy and cancer.[8, 9]

Lasers are particularly useful in the field of plastic surgery where minimally invasive procedures reduce scarring. In particular, lasers can be used to cause photocoagulation. Flash lamp pumped dye lasers are used to close small blood vessels, removing port wine stains.[6] Dermatologists have studied light penetration through the skin to understand more about the development of cancers, including melanoma, and photodermatosis (photoallergies).

The advent of phototherapy documented one of the first useful aspects of light penetration through skin. UVA and visible wavelengths of light have shown themselves beneficial in medical phototherapy due to their ability to penetrate human (or animal) skin. Phototherapy utilizes penetrating light to activate photosensitive chemicals in the skin. For example, psoralen, a photosensitive molecule, is used to treat psoriasis. Porfimer sodium and *meso*-tetra hydroxyphenyl chlorin are photosensitizers used to treat neoplasms in the oral cavity.[7] Antibody-targeted photolysis can also be used to selectively target and kill cells.[10] In addition to phototherapy, light provides beneficial chemical reactions in the skin, most notably the synthesis of vitamin D that requires light. The concept and development of transdermal photopolymerization emerged from the understanding of light penetration through skin and the desire to implant materials in a minimally invasive manner.

2.2.3 Photopolymerization in Medicine. While photopolymerizations have found many applications in industry, including wood varnishes and coatings, it has an even longer history in medicine. The first recorded medical use of light-induced polymerization was over 4000 years ago when Egyptians placed bitumen of Judea, containing unsaturated compounds, on linen strips for mummy preparation and subsequently placed the

mummies in sunlight for hardening.[11] Today, the dental community is responsible for extensive clinical use and research on photopolymerization.

Photopolymerizations are utilized in the field of dentistry for applications ranging from sealants for carie prevention to root canal procedures. Resins are placed in caries using photopolymerization. Bis-phenol-A-bis-(2-hydroxypropyl) methacrylate and tri(ethylene glycol) are typical monomers used in resins. The photopolymerization method is crucial to the successful restoration of the cavity to avoid resin shrinkage and good bonding to the tooth dentin.[12] Photocurable liners that are placed with the resin have been developed to aid resin bonding to the dentin.[13] Photopolymerizing resins are also used to fill root canals.[14] Lasers in the 400-500 nm light regime are clinically applied to photopolymerize in root canals.[14, 15] In additional, argon lasers have been coupled to optical fibers to allow photopolymerizations in endodontic therapy.[15] Research in photopolymerization of resins in root canals has examined the ability to photopolymerize through dentin. A low level argon laser is capable of photopolymerizing resin through millimeters of dentin from the root canal where a fiber optic is introduced.[15] Photopolymerization through dental ceramics has also been examined.[16]

New forms of light sources are being studied for the photopolymerization of resins that may prove useful for transdermal photopolymerization with cells. Pulsed lasers allow a more efficient photopolymerization that has a high conversion with less energy.[12, 17] Decreased energy exposure may prove useful in avoiding potential cellular damage when using transdermal photopolymerization for tissue engineering purposes.

Dentistry is also a good example of how photopolymerizations can be used to duplicate complex anatomical shapes. Teeth have complex sulcular regions that are difficult to duplicate. Research and clinical practice has shown how this complex sulcular morphology can be formed using commercial photopolymerizing resins in molds, providing functional and esthetic restorations.[18]

2.3 Methods

2.3.1 *Light Penetration.* Skin was shaven and harvested from all regions of a swine (Yorkshire, 6 months Massachusetts General Hospital). Fifteen samples of swine skin were excised and hair and fat were removed. Six samples of muscle and fat each were similarly prepared (approximately 1-cm squares). Eleven human cadaver skin samples (Caucasian, National Institute of Disease Research) ranging in thickness from 1.35 mm to 2.55 mm were cut into approximately 1 cm squares and the subcutaneous fat was removed. Tissue thickness was measured using a micrometer. Tissue hydration was maintained by a saline bath. An integrating sphere was connected to two monochromaters with a 75 W lamp (Spex Industries, Edison, NJ) as previously described.[19] The integrating sphere reflects the penetrated light equally in all directions so that the detector can then measure the intensity of the penetrated light at the wavelength selected by the monochromater. Synchronous scans were performed from 250-550 nm with 2 nm increments, 0.1 s integration time, 1 mm slits and 0 nm offset. The experimental apparatus is shown in Figure 2.3. Percent transmission was determined by dividing the detected transmitted light with tissue by the lamp synchronous scan

without tissue present (background). Linear regression analysis of light transmission versus sample thickness was performed using Minitab Software.

2.3.2 *Transdermal Photopolymerization Kinetics.* Differential scanning calorimetry (Perkin Elmer, DSC7 with a photocalorimetric accessory) was used to monitor the polymerization rate of PEODM to determined kinetic constants. The photocalorimetric accessory included a monochromator to select light of a given wavelength, as well as neutral density filters to control the incident light intensity. Polymerizations were monitored at 37°C in the presence of oxygen. In a typical experiment, 5-10 mg of the poly(ethylene oxide)-dimethacrylate (PEODM, MW 3400, Shearwater Polymers, 20% w/v in water) was placed in a DSC pan. A shutter was opened to expose the samples to light of the selected intensity and wavelength and the polymerization rate was obtained. A kinetic model developed and described elsewhere was used to predict the polymerization rates and double bond (functional group) conversion during the photopolymerization.[20] The model parameters were fit from the DSC rate data of PEODM using the method of Anseth et al.[21] Parameters used for both the UVA and visible light simulation were as follows: kinetic constant for propagation, 105 L/mol-s; monomer specific volume, 0.93 cc/g; polymer specific volume, 0.86 cc/g; thermal expansion coefficient of monomer, 0.0005 /°C, of polymer, 0.000075 /°C; Tg monomer, -100 °C; Tg polymer, 0 °C; concentration of initiator, 0.0025 M, monomer, 1 M. Visible light simulations used a calculated intensity of 20.69 mW/cm^2 (incident 100 mW/cm^2), initiator efficiency of 0.50 and fractional change in volume of 50 cc/g. UVA simulations used a calculated light intensity of 0.045 mW/cm^2 (incident 100 mW/cm^2), an initiator efficiency of 0.65 and a fractional change in volume of 150 cc/g. The kinetic model was

kindly provided by Dr. Kristi Anseth, University of Colorado, Boulder, (see Appendix A).

2.3.3 *Cellular biocompatibility.*

Mitochondrial metabolism. Primary bovine chondrocytes (preparation described in Sections 3.3.1 and 4.3.1) were plated at a density of $1x10^4$ cells/cc in 12-well tissue culture plates. Control wells consisted of no initiator or light and initiator only. HPK was added at desired concentrations from a stock solution (120 mg/ml). The plate was exposed to 1.5 mW/cm^2 UVA light for 2 minutes. After 24 hours media was removed and 1 ml MTT (1 mg/ml, [3-(4,5-dimethylthiazol-2-yl)-2,5-diphenyl-2H-tetrazolium bromide]) was added and incubated for 1-3 hours. One ml of 0.04 N HCl in isopropanol was added to the wells and mixed on a rotating shaker for 30 minutes. Absorbance was read at 560 nm (n=3).

Lipid Peroxidation. Primary bovine chondrocytes were placed in 12-well plates at a concentration of 1.5 millions cells/well. Each well contained 1 ml of media with 20% (w/v) PEG (Polysciences, MW 100,000). PEG was added to help dissolve the photoinitiator and to further duplicate the normal encapsulation procedure. Variables included control (no light or initiator), light only, 0.04, 0.1, 1.0 and 5.0% (w/v) photoinitiator 1-hydroxycyclohexyl phenyl ketone. Wells were exposed to 3 mW/cm^2 UVA light for 4 minutes. Two hundred microliters of cell supernatant was immediately taken from each well and 8-iso-PGF2alpha was directly assayed from the cell culture supernatant using an ELISA (R&D Systems).

2.3.4 *Albumin release*. A 5% (w/w) loading dose of albumin was encapsulated in the hydrogels. Bovine serum albumin (BSA, Sigma) was added to the 50/50% w/v

macromer solution of MW 1000 and vortexed. One hundred fifty microliter aliquots of albumin and polymer solution were placed in scintillation vials and photopolymerized 1 minute. Three millilters of PBS was added to the hydrogels. The gels (n=4) were incubated statically at 37°C. At various time points the PBS was removed and frozen while 3 mL fresh PBS was added. Albumin concentration in PBS was determined using a micro BCA assay (Pierce, Rockford, IL).

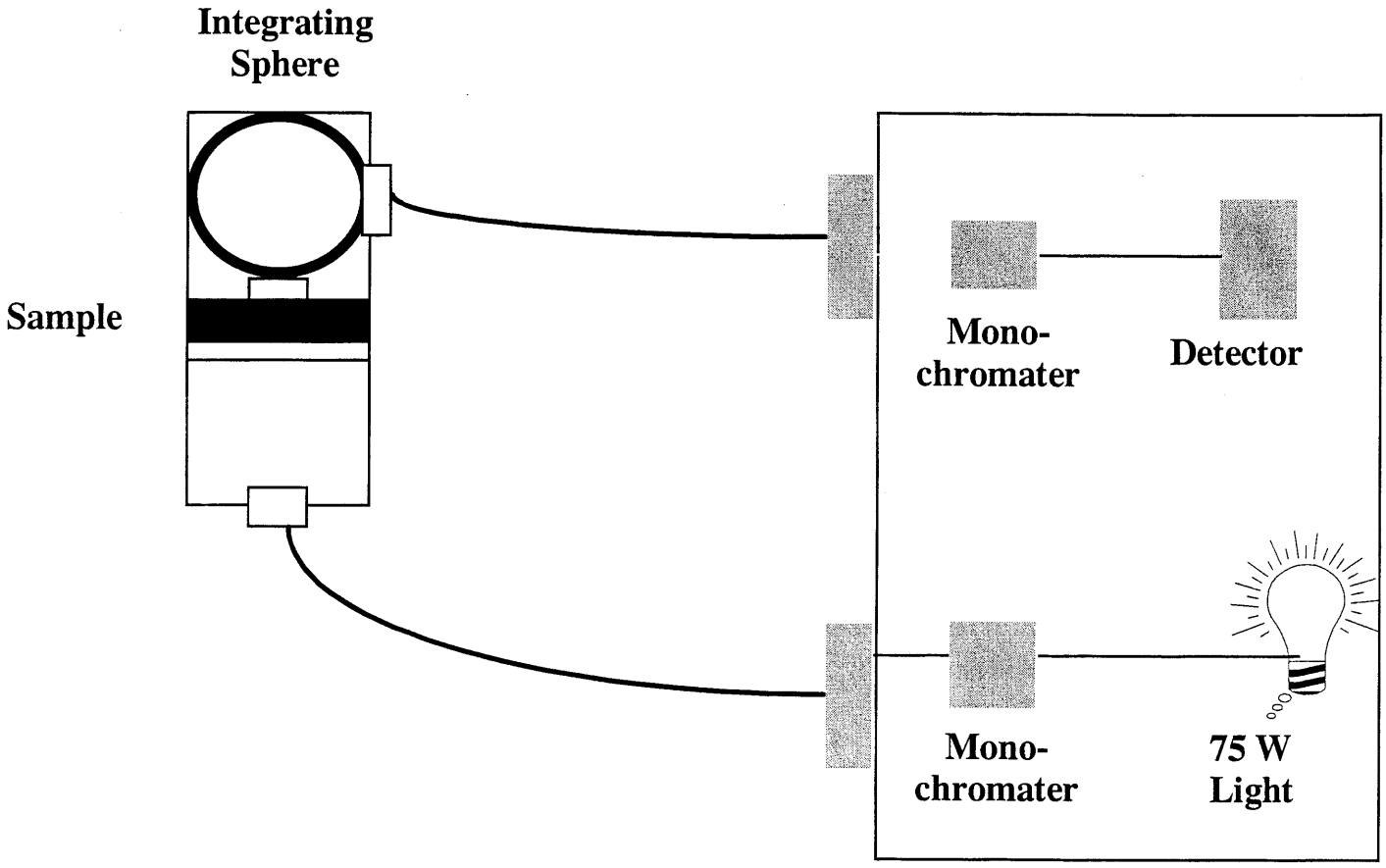

Figure 2.3. Experimental setup to study the penetration of light through tissue.

2.4 Results and Discussion

2.4.1 Light Penetration. The first feasibility issue for transdermal photopolymerization involved the ability of light to penetrate skin. Human skin ranges in thickness from 0.5 mm over the tympanic membrane and eyelids to 6 mm on the back and soles of feet and hands, with an average thickness of 1-2 mm.[22] While light transmittance has been examined in the stratum corneum and epidermis, few studies have focused on full thickness skin including the dermis.[19, 23] The penetration of light through full thickness skin is imperative since implants are generally placed beneath the dermis or even subcutaneous fat. The epidermis, typically only a fraction of 1 mm, contains chromophores that absorb radiation and impede the penetration of light. Collagen present in the dermis, which ranges in thickness throughout the body, is responsible for the majority of light attenuation in full thickness skin.[19, 23] Myoglobin in muscle and carotenes in fat are also capable of absorbing light. Figure 2.4 demonstrates the absorption of some common pigments found in animal tissues.

The transmittance of light through various tissue samples was analyzed from 300-550 nm. Figures 2.5 shows representative absorption spectra obtained from skin, muscle and fat samples analyzed from 300-500 nm. All tissues showed increasing light transmittance as wavelength increased. Skin absorbed more light than muscle and fat. Skin has developed methods (e.g., chromophores) to impede light penetration in order to protect an organism from light damage, particularly shorter wavelengths that can cause DNA and other damage. A peak of increased absorbance (or decreased light transmission) is present at 400 nm and is compatible with the absorption spectrum of hemoglobin. The hemoglobin peak is present in all of the tissue spectra. Thus it would

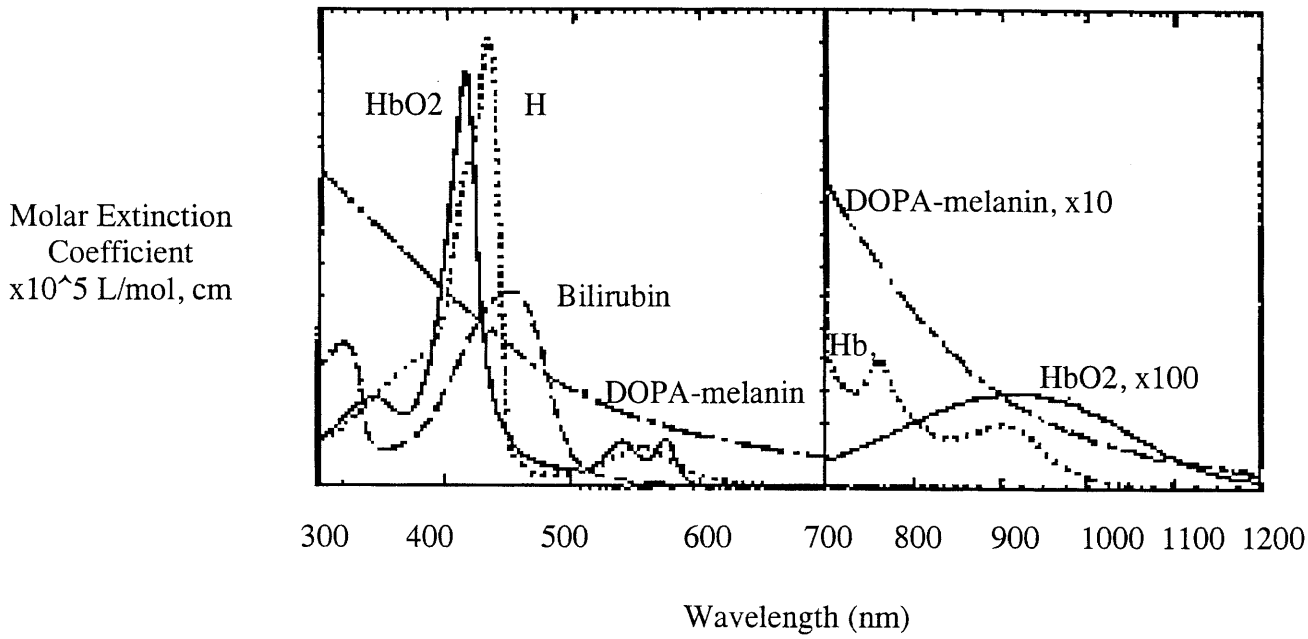

Figure 2.4. Absorption of various biological pigments (Parrish, J.A. in *The Science of Photomedicine*, eds. Regan, J.D. & Parrish, J.A., Plenum Press, New York, 1982).

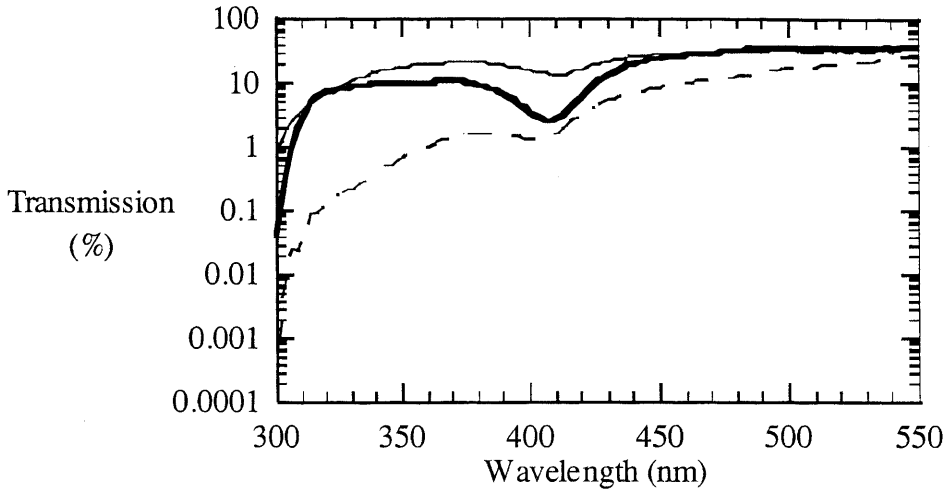

Figure 2.5. Transmittance of light through skin (---, 1.1 mm), muscle (-, 1.15 mm) and fat (-, 1.2 mm) from 300-550 nm.

be practical to avoid light and photoinitiators in the 400 nm wavelength range where hemoglobin will absorb light, decreasing transmittance.

The individual layers of the skin were separated to examine the individual transmission properties of each layer. Stratum corneum alone transmits the majority of exposed light (Figure 2.6). The dermis alone and full thickness skin samples demonstrate similar transmissions. This implies that the dermis is responsible for the majority of light attenuation in skin while the stratum corneum and epidermis readily allow light transmission.

Spectra from tissue samples of varying thickness were compiled at 360 and 550 nm. Figures 2.7 – 2.9 demonstrate the transmission of light through skin, muscle and fat respectively through tissue samples of varying thickness. The wavelengths 360 and 550 nm are in the ultraviolet (UVA) and visible light ranges respectively. Transmission data from these two wavelengths were compiled from the scans because common photoinitiators have maximal absorptions in these regions and they demonstrate bounds where transmission is low (360 nm) and high (550 nm). All skin samples exhibited decreasing light transmittance as tissue thickness increased and lower transmission in the UVA region of light. The trends were linear and statisically significant as demonstrated by regression analysis (Table 2.1)

Swine skin is often used as a model for human skin because of structural, functional and biochemical similarities.[24-26] Swine and human skin transmission was compared to verify the use of swine skin as a model for human skin. Longer wavelengths of light were able to penetrate deeper through the tissue similar as shown in the previous

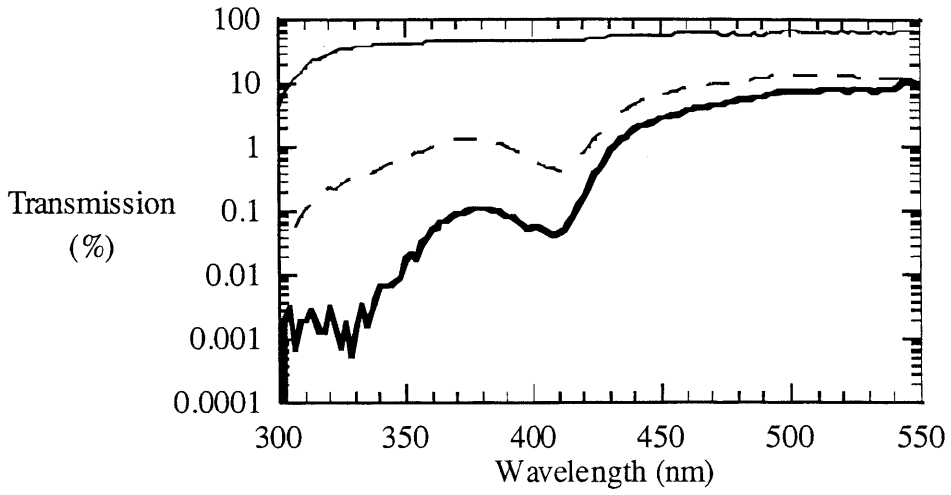

Figure 2.6. Transmittance of light through swine a.) stratum corneum and epidermis (-), b.) dermis alone (---, 1.99 mm) and c.) full thickness skin containing stratum corneum, epidermis and dermis (-, 2.2 mm) from 300-550 nm.

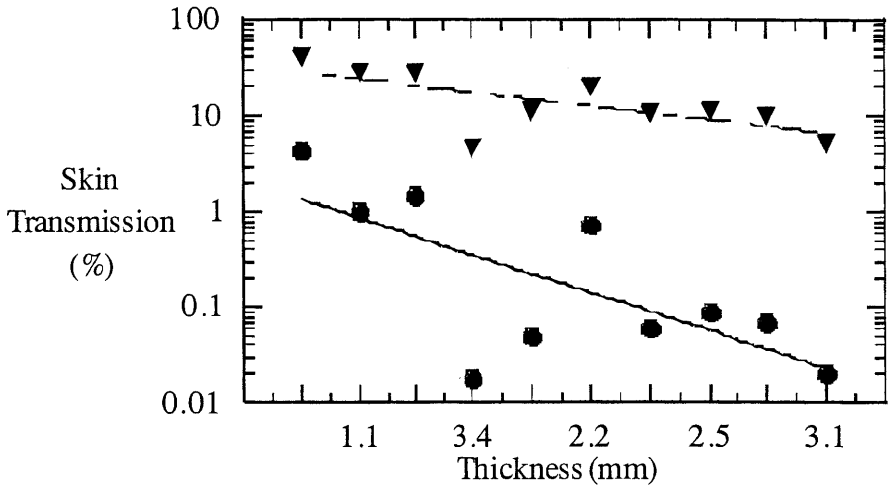

Figure 2.7. Transmittance of 360 (--l --) and 550 (--s --) nm light through full thickness swine skin of varying thickness.

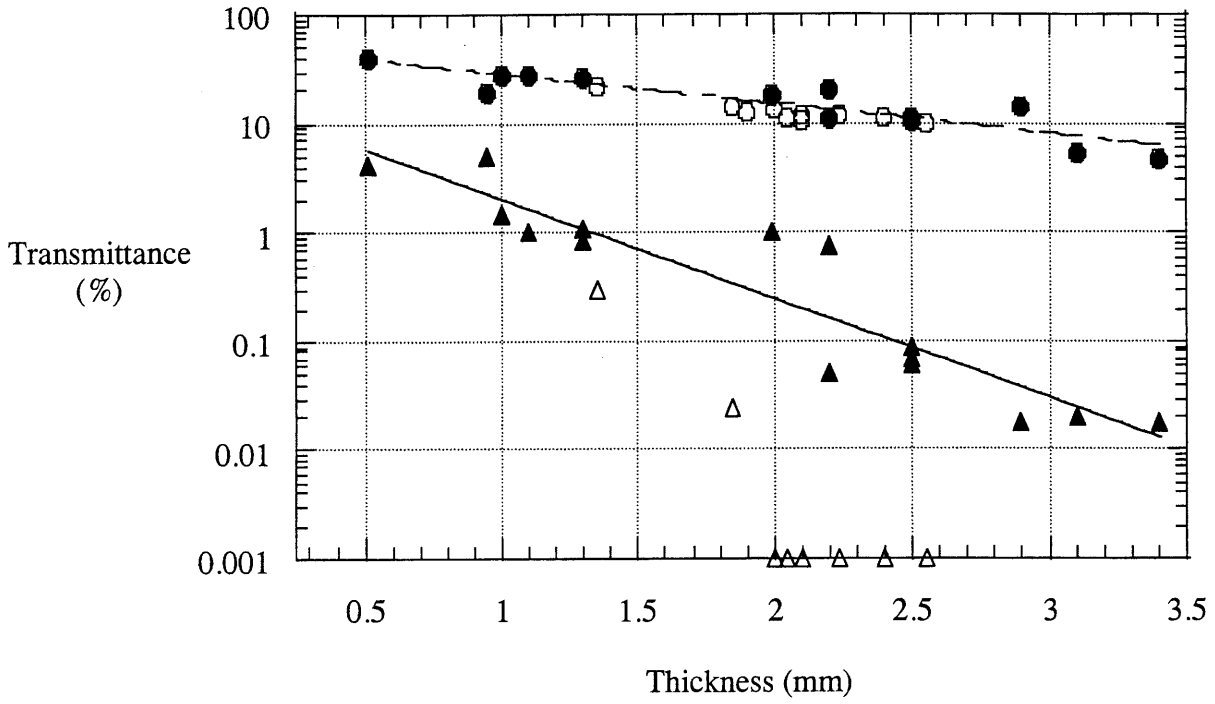

Figure 2.8. Penetration of light through swine skin at 360 (--s --) and 550 nm (--l --) and human skin at 360 (--D--) and 550 nm (--o--).

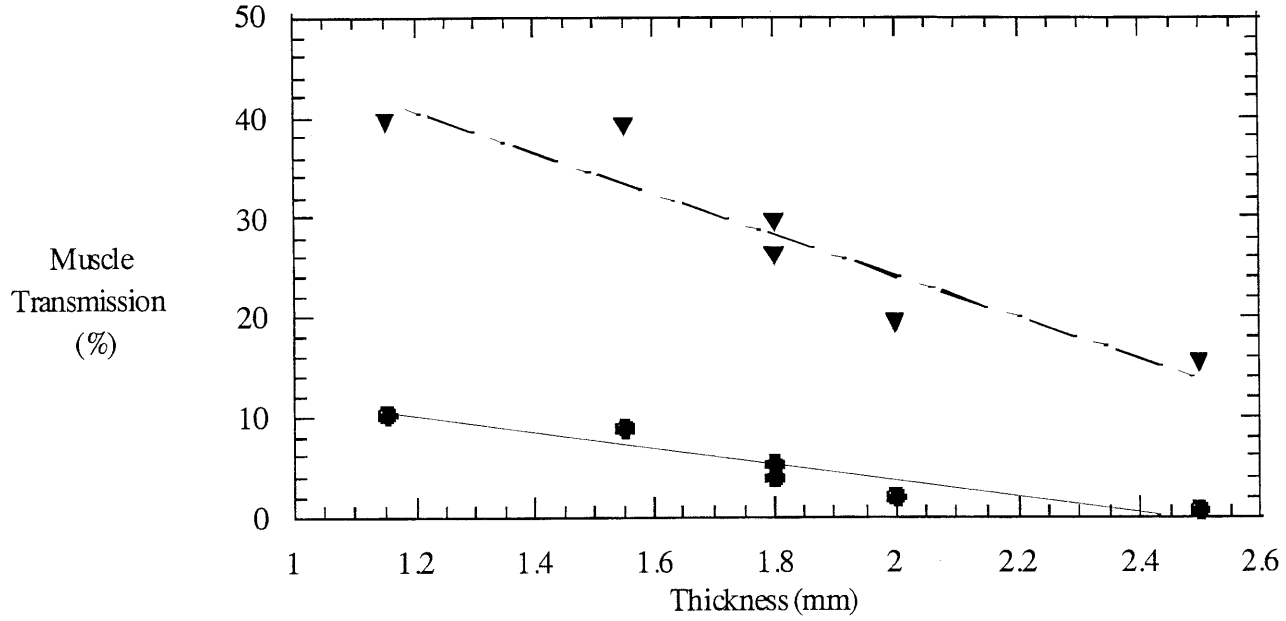

Figure 2.9. Transmittance of 360 (--l --) and 550 (--s --) nm light through swine muscle of varying thickness.

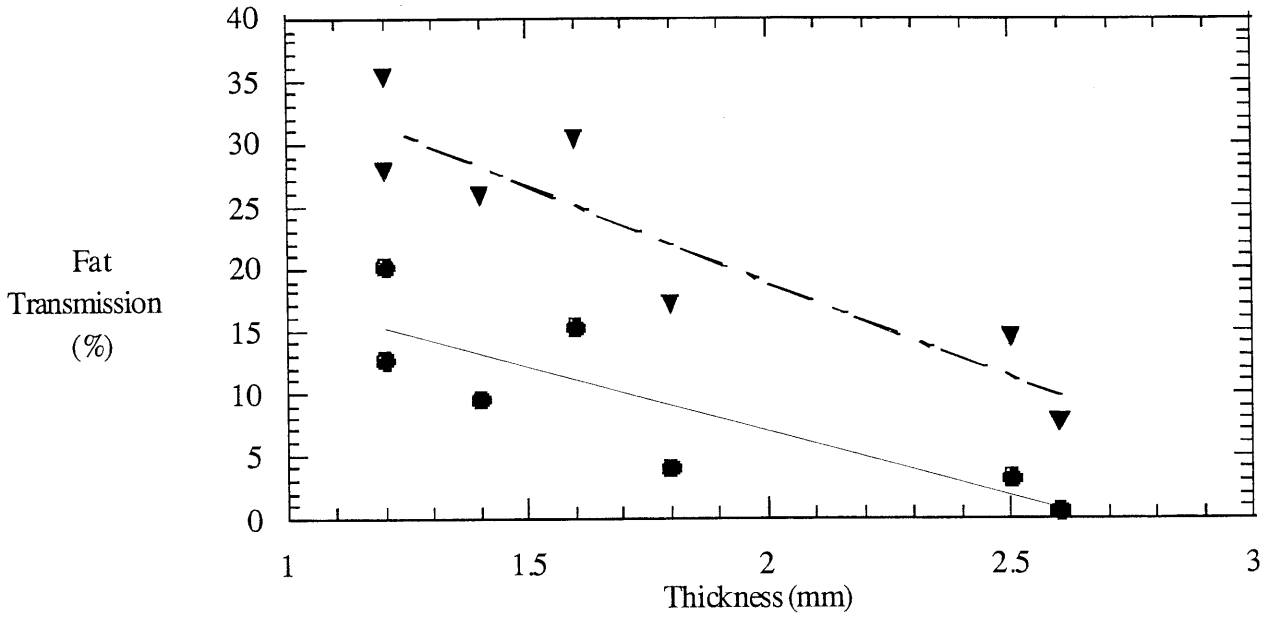

Figure 2.10. Transmittance of 360 (--l --) and 550 (--s --) nm light through swine subcutaneous fat of varying thickness.

experiment, but the transmittance of human skin in the UVA region was markedly reduced compared to swine skin (Figure 2.8). Negligible UVA light penetrated human skin greater than 2 mm in thickness. Human and swine skin demonstrated similar absorption in the visible light region analyzed (400-550 nm, Figure 2.8). Thus, swine skin provides an appropriate model for light transmittance through human skin in the visible light range only. The increased penetration of visible light, particularly in human skin, suggests that the efficiency and toxicity of visible light photoinitiators should be investigated for transdermal photopolymerization in humans.

2.4.2 Kinetics. The time required to transdermally photopolymerize a hydrogel under skin was examined using a kinetic model for photopolymerization. Figure 2.11 portrays the conversion versus time of PEO-dimethacrylate (PEODM, MW 3400) under 1.5 mm human skin using visible or UVA light. A control reaction, with no skin present, is shown using a UVA light source. An incident light intensity of 100 mW/cm^2 (used clinically in phototherapy) and 0.04% (w/w) photoinitiator were used for the simulations.[27] UVA photoinitiators have a higher efficiency than visible light photoinitiators, yet the penetration of visible light through human skin is greatly enhanced compared to UVA radiation (Figure 2.11).[28] The primary influence of light attenuation in tissue is a decrease in polymerization rate and an increase in polymerization time. While the conversion of PEODM beneath human skin using visible and UVA radiation does not largely differ after 15 minutes (900 s), the visible light polymerization reaches over 80% conversion (and has formed a mechanically stable network) after only 100 s of skin exposure to light. Even under skin with minimal light

	Regression p-values	
	360 nm	550nm
Skin	0.004	$<10^{-4}$
Muscle	0.005	0.008
Fat	0.016	0.004

Table 2.1. Table of p-values for linear regressionanalysis of light penetration through skin, muscle and fat.

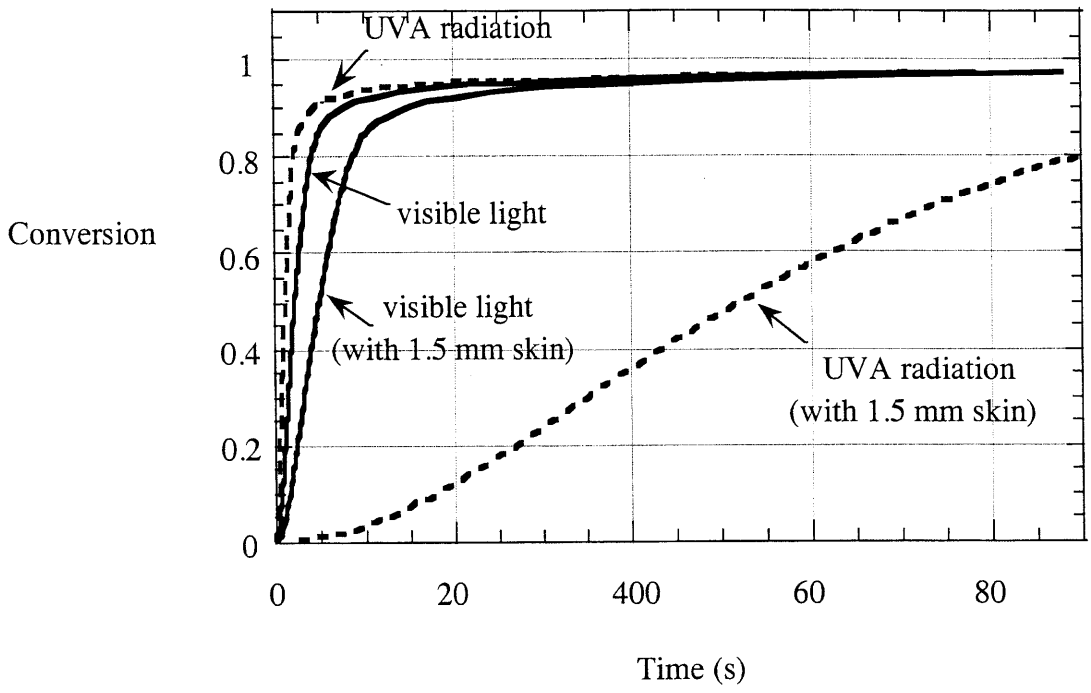

Figure 2.11. Kinetics of transdermal photopolymerization of PEODM with UVA (--), visible light (?) and beneath 1.5 mm human skin using UVA (--) and visible light (?) using an incident light intensity of 100 mW/cm^2 and 0.04 % (w/w) photoinitiator.

transmittance, polymerization times required for transdermal photopolymerization under skin are short, clinically feasible times, on the order of minutes (Figure 2.12).

The effect of tissue thickness on polymerization time was determined using the light transmission data from Figures 2.7 - 2.9 and the kinetic modeling program. Figure 2.12 shows the time required to reach 90% conversion under skin, fat and muscle of varying thickness. This information will be useful for *in vivo* implantation using transdermal photopolymerization. With knowledge of the desired depth of implantation, the light exposure time required for polymerization can be determined

2.4.3 Cellular biocompatibility

Mitochondrial metabolism. To examine the cellular toxicity of transdermal photopolymerization, we studied the effects of the activated photoinitiator on chondrocyte (a model cell for tissue engineering) metabolism. The worst case scenario of all radicals available to damage cells was examined by excluding the polymer, which reacts with the radical species formed by photoinitiator exposure to light. Figure 2.13 demonstrates the effect of increasing photoinitiator concentration (HPK, 1-hydroxycyclohexyl phenyl ketone) in complete media on cell metabolism as determined by MTT activity located in the mitochondria and cytoplasm. A decrease in chondrocyte MTT activity with increasing HPK concentration is observed after exposure of the cells and initiator to light compared to controls (Figure 2.13). Low photoinitiator concentrations (0.01-0.04% w/v) caused minimal chondrocyte damage, yet still allowed photopolymerization to occur as demonstrated in the polymerization kinetics in Figure

2.11. These initiation conditions were subsequently utilized for optimal cell encapsulation using photopolymerization.

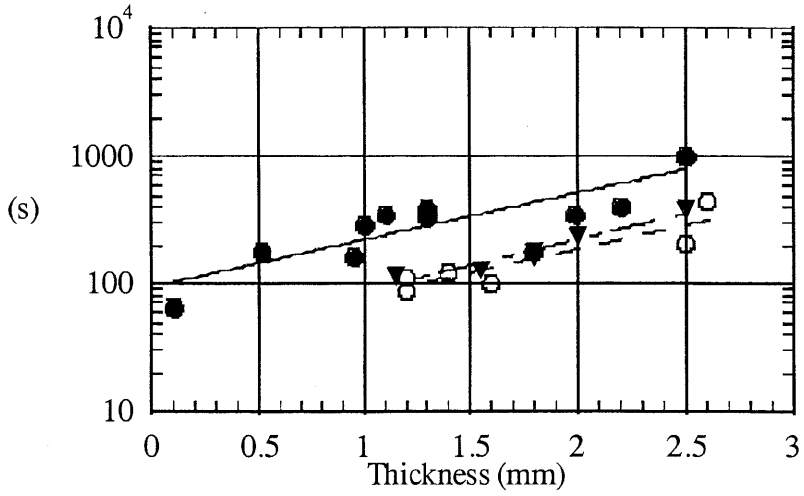

Figure 2.12. Time required for 90% conversion under varying thickness swine skin (--I --), muscle (--D--) and fat (--o--) using an incident light intensity of 100 mW/cm^2 and 0.04% (w/w) photoinitiator.

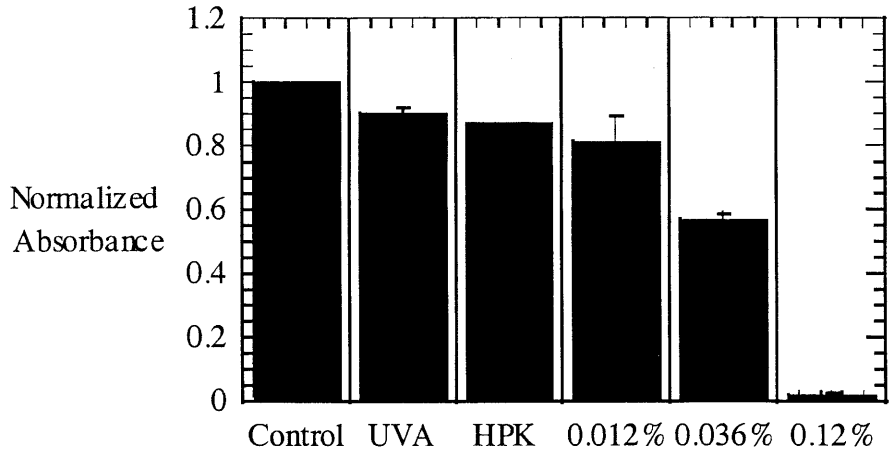

Figure 2.13. Normalized MTT absorbances of chondrocytes after exposure to 1.5 mW/cm^2 UVA light and HPK (% w/v). Control cells were not exposed to initiator or light, HPK control (0.036% HPK) was not exposed to light and UVA control cells were exposed to light only.

Lipid Peroxidation. Initial biocompatibility studies used MTT to examine cellular metabolism after exposure to the photoinitiator. These studies demonstrated that increasing photoinitiator concentrations caused a decrease in cell viability although a minimal photoinitiator concentration showed no difference from control cells. While MTT provided an initial screening for photoinitiators, it is not a sensitive probe or potential oxidative damage. The first region of a cell that a radical produced by a photoinitiator in solution will encounter is the cell membrane. Lipids containing arachidonic acid (e.g. present in the cell membrane and plasma) may undergo a free radical-catalyzed reaction to form prostaglandin-F_2 compounds.[29] Furthermore, lipid peroxidation caused by photoinitiators has been examined by groups in the dental community.[30, 31] Prostaglandin-F_2 compounds have biological activity when released from cells *in vivo* and can further react with cell components causing protein and DNA oxidative damage.[32] The prostaglandin-F_2 compounds are the source of the majority of malondialdehyde that is capable of reacting with DNA and is measured in the thiobarbituric acid test, the classic test for oxidative stress or damage.[29] The formation of prostaglandin-like compounds from arachidonic acid by oxidative stress is depicted in Figure 2.14.

The chondrocytes exposed to the photoinitiator HPK exhibited higher levels of 8-iso-PGF_2alpha compared to control wells (Figure 2.15). The 0.04% wells produced approximately four times the quantity of 8-iso-PGF_2alpha. The 1.0% HPK wells produced even more 8-iso-PGF_2alpha while concentrations decreased in the 5% HPK wells. This decrease in 8-iso-PGF_2alpha production with a higher concentration of HPK may be caused by the decrease in cell viability (as demonstrated by the MTT results) and

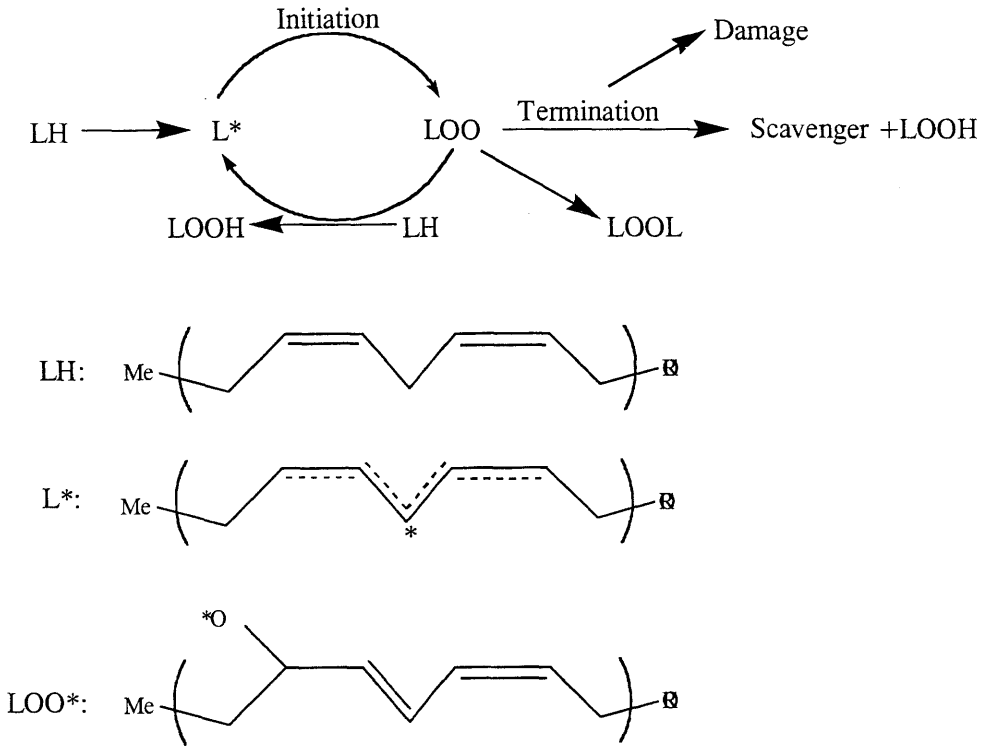

Figure 2.14. General reaction scheme of a lipid exposed to a radical. Adapted from: "Free Radical Damage and its Control" in New Comprehensive Biochemistry vol.28, eds. Rice-Evans, C.A. and Burdon, R.H.

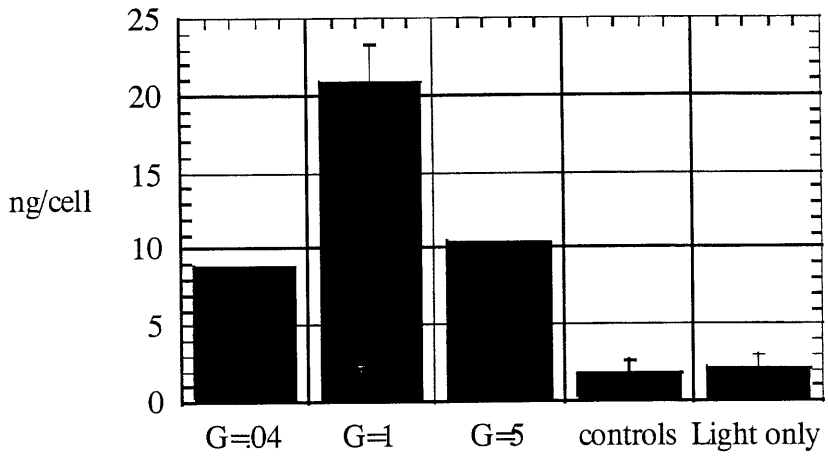

Figure 2.15. Concentration of 8-iso-PGF_2alpha in cell super-natent of chondrocytes exposed to 0.04, 1 and 5% HPK, light without HPK and controls exposed to neither light or HPK.

disruption of the cell membrane. Chondrocytes exposed to UVA light (without HPK) had similar 8-iso-PGF_2alpha levels to controls.

Potential radical cell damage may be overcome by various methods. Various initiators and their toxicity can be examined. Furthermore, the initiator may be attached to the macromer, limiting its mobility and potentially ability to react with cells. Post polymerization and radical damage, various additives such as glutathione may be provided in the hydrogel to promote repair of potential oxidative stress damage.

2.4.4 Tissue Biocompatibility. Hydrogels without chondrocytes were implanted via transdermal photopolymerization to observe the tissue response to implantation and the semiIPN. Figure 2.16 shows the skin, subcutaneous tissue and hydrogel in a mouse 3 days after implantation. No light damage, characterized by pyknotic nuclei, is observed in the skin. The implanted polymer is surrounded by a fibrous capsule with inflammatory cells (polymorphonuclear leukocytes, lymphocytes and giant cells), demonstrating a foreign body response comparable to other biomaterials such as PGA.[33] These experiments suggest biocompatibility of the transdermal photopolymerization process and the hydrogel implant. Similar polymer hydrogels have been photopolymerized *in situ* in clinical trials for adhesion prevention after surgery in the abdomen and as a sealant in the lungs.[3]

2.5 Applications

One envisioned application for transdermal photopolymerization and simultaneous photoencapsulation of cells is tissue engineering. A minimally invasive technique to tissue engineer cartilage would provide many benefits in plastic surgery.

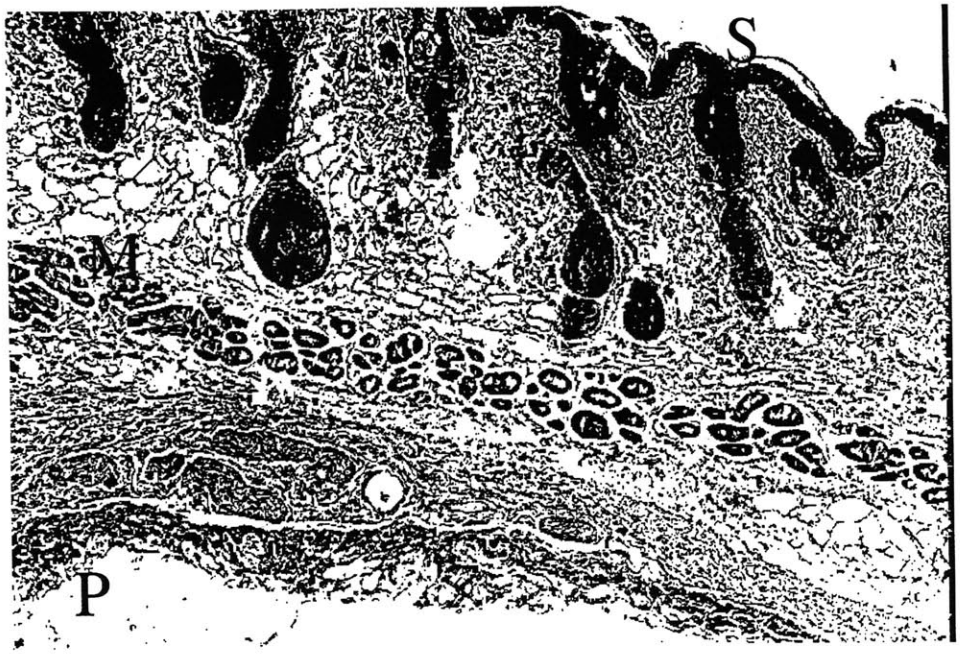

Figure 2.16. H&E stained section of an implanted hydrogel (P, without cells), surrounded by a fibrous capsule (C), subcutaneous tissue and skin (S).

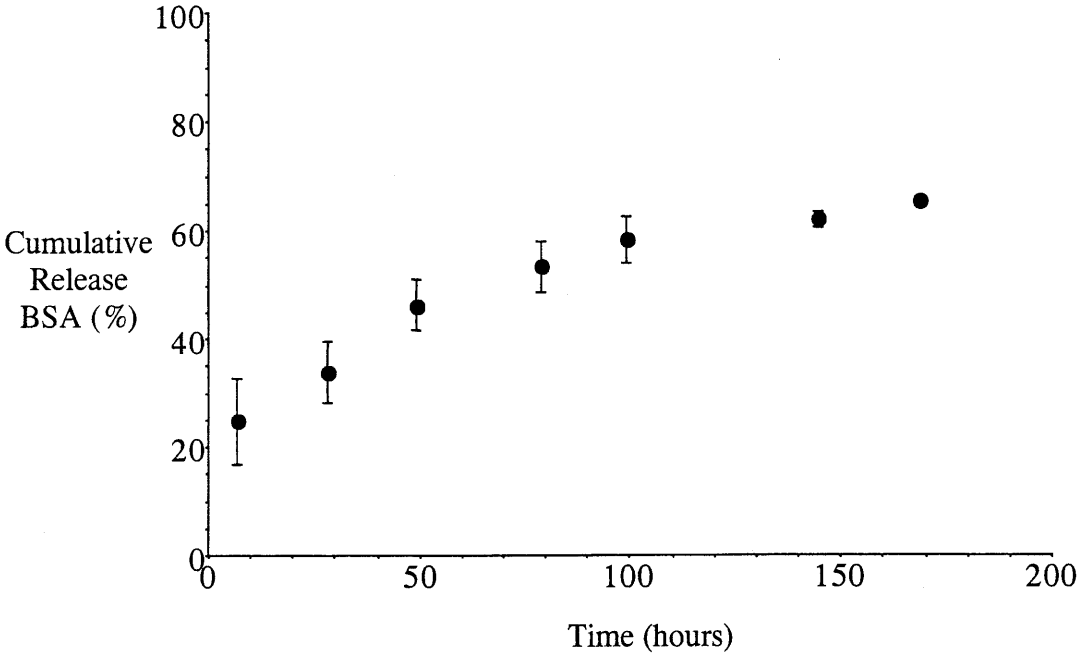

Figure 2.17. Release of BSA from PEODM (MW1000) hydrogels over 200 hours.

For example, cell and macromer solutions could be injected underneath the skin, molded to the desired shape, and subsequently photopolymerized circumventing the need for any surgical incisions. The cartilage formed from the *in situ* molded and polymerized gel would be beneficial for augmentation reconstructive surgeries. The potential of transdermal photoencapsulation of chondrocytes for tissue engineering will be discussed in Chapters 3-5.

In addition to the potential applications in tissue engineering, transdermal photopolymerization may potentially be applied to the implantation of polymers for drug delivery. Transdermal photopolymerization would allow physicians to implant polymer delivery devices without the need for surgical intervention, thus providing an inexpensive method with reduced risk to the patient and potentially newfound applications. In contrast to methods that inject microparticles, these monolithic devices would potentially have minimal migration, maintain localized delivery, and could be easily removed if needed. As an illustration for this application, bovine serum albumin (BSA, MW 6800) was photopolymerized in PEODM hydrogels (MW1000) and release was observed for the duration of the experiment (Figure 2.17). In addition, other cell types may potentially be encapsulated to secrete a drug or for engineering other tissues types.

2.6 References

1. Hill-West, J., Chowdhury, S., Slepian, M. & Hubbell, J., Inhibition of thrombosis and intimal thickening by in situ photopolymerization of thin hydrogel barriers. *Proc Natl Acad Sci USA* **91**, 5967-71 (1994).

2. Hill-West, J., Dunn, R. & Hubbell, J., Local release of fibrinolytic agents for adhesion prevention. *J Surg Res* **59**, 759-63 (1995).

3. Sawhney, A., Lyman, F., Yao, F., Levine, M. & Jarrett, P. in *23rd International Symposium of Controlled Release of Bioactive Materials* 236-237 (Controlled Release Societym Inc., Kyoto, Japan, 1996).

4. Watts, D.C. in *Materials Science and Technology: A Comprehensive Treatment* (ed. Williams, D.F.) 209-258 (VCH Publishers, New York, NY, 1992).
5. Peppas, N. Hydrogels in Medicine and Pharmacy, CRC Press, Boca Raton, FL, 1987.

6. Bown, S.G., New Techniques in Laser Therapy. *BMJ* **316**, 754-7 (1998).
7. Spencer, G., *et al.*, Laser and brachytherapy in the palliation of adenocarcinoma of the oesophagus and gastric cardia. *Gut* **39**, 726-31 (1996).

8. Amin, Z., *et al.*, Hepatic metastasis: interstitial laser photocoagulation with real time ultrasound monitoring and dynamic CT evaluation of treament. *Radiology* **187**, 339-47 (1993).

9. De la Rosette, J., Muschter, R., Lopez, M. & Gillat, D., Interstitial laser coagulation in the treatment of benign prostatic hyperplasia using a diode laser system with temperature feedback. *Br J Urol* **80**, 433-8 (1997).

10. Oseroff, A.R., Ohuoha, D., Hasan, T., Bommer, J.C. & Yarmush, M.L., Antibody-targeted photolysis: Selective Photodestruction of Human T-cell Leukemia Cells using Monoclonal Antibody-chlorin e6 Conjugates. *PNAS* **83**, 8744-8748 (1986).

11. Decker, C., UV-Curing Chemistry: Past, Present and Future. *Journal of Coatings Technology* **59**, 97-106 (1987).

12. Tarle, Z., *et al.*, The effect of the photopolymerization method on the quality of composite resin samples. *J Oral Rehabil* **25**, 436-42 (1998).

13. Nikaido, T., Formulation of photocurable bonding liner and adhesion to dentin. Effect of photoinitiator, monomer and photoirradiation. *Shika Zairyo Kikai* **8**, 862-76 (1989).

14. Potts, T. & Petrou, A., Argon laser initiated resin photopolymerization for the filling of root canals in human teeth. *Lasers Surg Med* **11**, 257-62 (1991).

15. Potts, T. & Petrou, A., Laser photopolymerization of dental materials with potential endodontic application. *J Endod* **16**, 265-8 (1990).

16. Le Denmat, D., Estrade, D. & Fleiter, B., Photopolymerization through ceramic. *Rev Fr Prothes Dent* **17**, 39-45 (1990).

17. Meniga, A., Tarle, Z., Ristic, M., Sutalo, J. & Pichler, G., Pulsed blue laser curing of hybrid composite resins. *Biomaterials* **18**, 1349-54 (1997).

18. Liebenberg, W., Occlusal index-assisted restitution of esthetic and functional anatomy in direct tooth-colored restoration. *Quintessence Int* **27**, 81-8 (1996).

19. Anderson, R.R. & Parrish, J.A. in *The Science of Photomedicine* (eds. Regan, J.D. & Parrish, J.A.) 147-194 (Plenum Press, New York, 1982).

20. Anseth, K.S. & Bowman, C.N., Kinetic Gelation Model Predictions of Crosslinked Polymer Network Microstructure. *Chemical Engineering Science* **49**, 2207-2217 (1994).

21. Anseth, K., Wang, C. & Bowman, C., Reaction behavior and kinetic constants for photopolymerizations of multi(meth)acrylate monomers. *Polymer* **35**, 3243 (1994).

22. Woodburne, R.T. & Burkel, W.E. *Essentials of Human Anatomy* (Oxford University Press, New York, 1994).

23. Bruls, W., Slaper, H., van der Leun, J. & Berrens, L., Transmission of Human Skin Epidermis and Stratum Corneum as a Function of Thickness in the Ultraviolet and Visible Wavelengths. *Photochemistry and Photobiology* **40**, 485-494 (1984).

24. Walker, M., *et al.*, In vitro model for percutaneous delivery of active repair agents. *J Pharm Sci* **86**, 1379-1384 (1997).

25. Meyer, W., Comments on the suitability of swine skin as a biological model for human skin. *Hautarzt* **47**, 178-182 (1996).

26. Fourtanier, A. & Berrebi, C., Miniature pigs as an animal model to study photoaging. *Photochem Photobiol* **50**, 771-784 (1989).

27. Parrish, J.A. in *The Science of Photomedicine* (eds. Regan, J.D. & Parrish, J.A.) 3-18 (Plenum Press, New York, 1982).

28. Odian, G. *Principles of Polymerization* (John Wiley & Sons, Inc., New York, 1991).

29. Morrow, J.D. & Roberts, L.J., Quantification of Noncyclooxygenase Derived Prostanoids as a Marker of Oxidative Stress. *Free Radical Biology & Medicine* **10**, 195-200 (1991).

30. Terakado, M., *et al.*, Lipid peroxidation as a Possible Cause of Benzoly Peroxide Toxicity in Rabbit Dental Pulp-a Microsomal Lipid Peroxidation *in vitro*. *J Dent Res* **63**, 901-905 (1984).

31. Fujisawa, S., Kadoma, Y. & Masuhara, E., Effect of Photoinitiators for the Visible-light Resin System on Hemolysis of Dog Erythrocytes and Lipid Peroxidation of Their Components. *J Dent Res* **65**, 1186-1190 (1986).

32. Park, J.-W. & Floyd, R.A., Lipid Peroxidation Products Medi
ate the Formation of 8-hydroxydeoxyguanosine in DNA. *Free Radical Biology & Medicine* **12**, 245-250 (1992).

33. Anderson, J.M., Inflammatory Response to Implants. *Trans. Am. Soc. Artif. Intern Organs* **XXXIV** (1988).

Chapter 3. *In vitro* Photoencapsulation of Chondrocytes in PEO-based Hydrogels*.

3.1 Introduction

This chapter explores the ability to encapsulate chondrocytes *in vitro* in a hydrogel using a photopolymerization. Current methods for encapsulating cells in gels are reviewed. The production of collagen and glycosaminoglycans, the two major components of cartilage extracellular matrix, was examined in order to demonstrate the potential use of photoencapsulation for cartilage tissue engineering purposes.

3.2 Background

Tissue engineering has developed as a potential method to replace cartilage tissue lost from trauma, tumor resection, congenital malformations or various disease processes.[1] Cartilage tissue engineering has been an area of intense research due to the lack of regenerative capacities of cartilage *in vivo* and the limited options currently available clinically to replace cartilage structure and function. The tissue engineering potential of a new scaffold or encapsulation system is often examined first *in vitro* to observe cell responses in a controlled environment.

Cartilage is composed of chondrocytes distributed within an extracellular matrix. The extracellular matrix is maintained by the chondrocytes and is comprised of negatively charged proteoglycans, or glycosaminoglycans, which provide compressive strength, and a collagen network that provides tensile strength.[2] The purpose of tissue

* This chapter will be submitted in part for publication in a peer-reviewed journal

engineering is to provide an environment and appropriate signals that will stimulate chondrocytes to synthesize and form an organized extracellular matrix similar to native cartilage. Current methods for tissue engineering cartilage use scaffolds, both synthetic and biological, to create an environment to promote tissue formation. Scaffolds provide important functions including mechanical support for developing tissue while allowing for diffusion of nutrient and waste products.[3] In addition, scaffolds provide a matrix on which cells may adhere and multiply as in the case of solid scaffolds, or physically entrap cells in the case of liquid and gel scaffolds.

Both solid and liquid gel scaffolds have been studied as potential matrices for cartilage tissue engineering. Solid scaffolds include poly(glycolic acid), PGA, meshes which have been successfully used to engineer cartilage both *in vitro* and *in vivo*.[3] Recent attention has focused on engineered cartilage systems that can be injected in a noninvasive manner for use in arthroscopic surgery.[4] A liquid scaffold system may be injected arthroscopically or through a needle for subcutaneous implantation.

To design an injectable system, polymer scaffolds must be identified or developed that are: i) water soluble to produce cell-polymer suspensions and ii) undergo a physical or chemical change causing gelation after injection. Current gelling systems under investigation include alginate, Pluronics, and fibrin glue. Alginate, a polysaccharide, forms an ionic network in the presence of divalent or multivalent ions. Many groups have investigated the activity and biological properties of chondrocytes entrapped in alginate *in vitro*.[5] Alginate has been examined *in vivo* for use in craniofacial cartilage replacement and as cartilage plugs to prevent vesicoureteral reflux.[6, 7] Similarly, chondrocytes have been encapsulated in agarose gels and the biochemical and

mechanical properties of the resulting tissue has been studied.[8] Fibrin glue is another biological gel which has been used to encapsulate chondrocytes but the resulting gel degrades too quickly to maintain structural integrity before tissue is formed.[9]

The purpose of this chapter is to analyze *in vitro* the potential of an injectable polymer system that would encapsulate chondrocytes in a fast, controllable manner and promote cartilage formation. Substituted poly(ethylene oxide) and a photopolymerization process were utilized to transform a liquid, polymer solution to a gel. The biochemical and mechanical properties of the resulting tissue were studied.

3.3 Methods

3.3.1 Cell Isolation. Saddle sections from 1-2 week-old calves were obtained from a local abbattoir (A. Arena, Hopkington, MA). The intact femoropatellar groove was removed and chondrocytes were immediately isolated using type II collagenase (0.2% in complete media with overnight incubation, Worthington, Freehold, NJ), washed three times with phosphate buffered saline (PBS) and passed through a Nytex filter. Ovine chondrocytes were obtained from ovine saddle sections in a similar manner. Cell number was determined by hemocytometer counting. Cells were centrifuged (1000 rpms, 10 minutes) to form a pellet prior to the addition of polymer.

3.3.2 Polymer Preparation. Poly(ethylene oxide), PEO (100,000, Shearwater Polymers, Knoxville, TN) and poly(ethylene oxide)-dimethacrylate, PEODM (3400, Shearwater Polymers) were combined in a 3:2 ratio and dissolved in PBS (phosphate buffered saline with 100 U/ml penicillin G, 100 μg/ml streptomycin) to form a 20% (w/v) solution. The photoinitiator 1-cyclohexyl phenyl ketone (HPK, Polysciences) was added to the polymer

solution (3μl/ml polymer solution from a stock of 120 mg/ml in 70% ethanol). After thorough mixing to dissolve the polymer, the solution was added to a pellet of chondrocytes to make a final concentration of $50x10^6$ cells/cc. The chondrocytes were suspended in the viscous polymer solution by thorough mixing.

3.3.3 Photopolymerization. One hundred fifty microliters of the chondrocyte/polymer suspension was placed in either sterile Eppendorfs or tissue culture inserts (diameter 6 mm) and placed under a UVA lamp for 3 minutes (Fig.3.1). The lamp was at a height so that the polymer/chondrocyte solutions received a light intensity of approximately 2-3 mW/cm^2 as determined by radiometer measurements. Resulting hydrogels were removed from the Eppendorf or tissue culture insert using a sterile spatula and placed in 12-well tissue culture plates with media (high glucose DMEM, 10% FBS, 10 μg/ml vitamin C, 12.5 mM HEPES, 0.1 mM nonessential amino acids and 0.4 mM proline). Media was refreshed biweekly. Hydrogels were incubated statically at 37°C, 5% CO_2. Control hydrogels were synthesized and incubated as described above but contained only polymer (without chondrocytes).

3.3.4 Biochemical Characterization. Hydrogels were analyzed by MTT ([3-(4,5-dimethylthiazol-2-yl)-2,5-diphenyl-2H-tetrazolium bromide]) and light microscopy one day after chondrocyte encapsulation. Three milliliters of MTT (0.5 mg/ml in DMEM with 2% FBS) were added to hydrogels in 12-well plates. The hydrogels and MTT were incubated for 2 hours. The MTT solution was removed and the hydrogels were rinsed twice with PBS and micrographs (4.5X magnification) were obtained.

Biochemical analysis was performed on hydrogel constructs formed in Eppendorfs with bovine chondrocytes after 3, 7, 10 and 14 days of incubation. Hydrogels without

cells were used as controls. Constructs were removed from the tissue culture plates, blotted dry and wet weights (ww) were obtained. Gels were subsequently lyophilized for at least 48 hours after which dry weights (dw) were determined. The hydrogels were digested in 1 ml papainase overnight at 60°C. GAG content was estimated by chondroitin sulfate using dimethylene blue dye and a UV-VIS spectrophotometer.[10] Total collagen content was determined by the hydroxyproline determined after acid hydrolysis and reaction with p-dimethylaminobenzaldehyde and chloramine-T using 0.1 as the ratio of hydroxyproline to collagen.[11] The cell content of the hydrogels was determined using Hoechst 33258, spectrofluorometry and a conversion factor of 7.7 pg DNA per chondrocyte.[12]

The polymer content of the hydrogel constructs was estimated from the biochemical data. GAG and collagen contents (dry weights) were subtracted from the construct total dry weight in order to estimate the polymer dry weight remaining in the constructs. The remaining polymer is expressed as a percentage of the construct wet weight. Control hydrogels (n=5) were synthesized as described, washed and vacuum dried to determine original dry weight. The controls were then placed in media and incubated at 37°C. Control polymer contents after incubation were determined from media sampling. All of the media bathing the hydrogels was removed at specified time points and vacuum dried. The weight of dried media alone was subtracted from the media samples of the hydrogels. The amount of polymer present in the media was expressed as percentage of the original hydrogel dry weight. One-way statistical analysis of variance (ANOVA) was performed using Minitab.

Histology was performed on hydrogels incubated for 2 weeks. The hydrogels were preserved in 10% formalin and prepared according to standard histological technique. Sections were stained with hematoxylin and eosin (H&E) and SafraninO.

3.3.5 Mechanical Characterization. Hydrogels were photopolymerized in tissue culture inserts with ovine chondrocytes for mechanical analysis in order to form constructs in a disk shape. 40% PEODM and 100% PEODM control gels without cells were prepared the day before testing and allowed to swell overnight in PBS. Hydrogel constructs with cells were incubated at 37°C, 5% CO_2 and analyzed after 3 and 6 weeks of incubation. Six-mm diameter disks were cored from the hydrogels that averaged approximately 7-8 mm in diameter. Thickness was measured by a current-sensing micrometer and was generally on the order of 1.5 mm.

Mechanical and electromechanical properties were measured in uniaxial confined compression in an apparatus described previously.[8] The equilibrium stress-strain behavior was assessed by stepwise compressions of 10, 20 and 30% and load was recorded for 15 minutes. After stress relaxation reached equilibrium at the 30% static offset, a dynamic compression was superimposed at a frequency of 0.01-1 Hz. The resulting oscillatory load and streaming potential were detected.

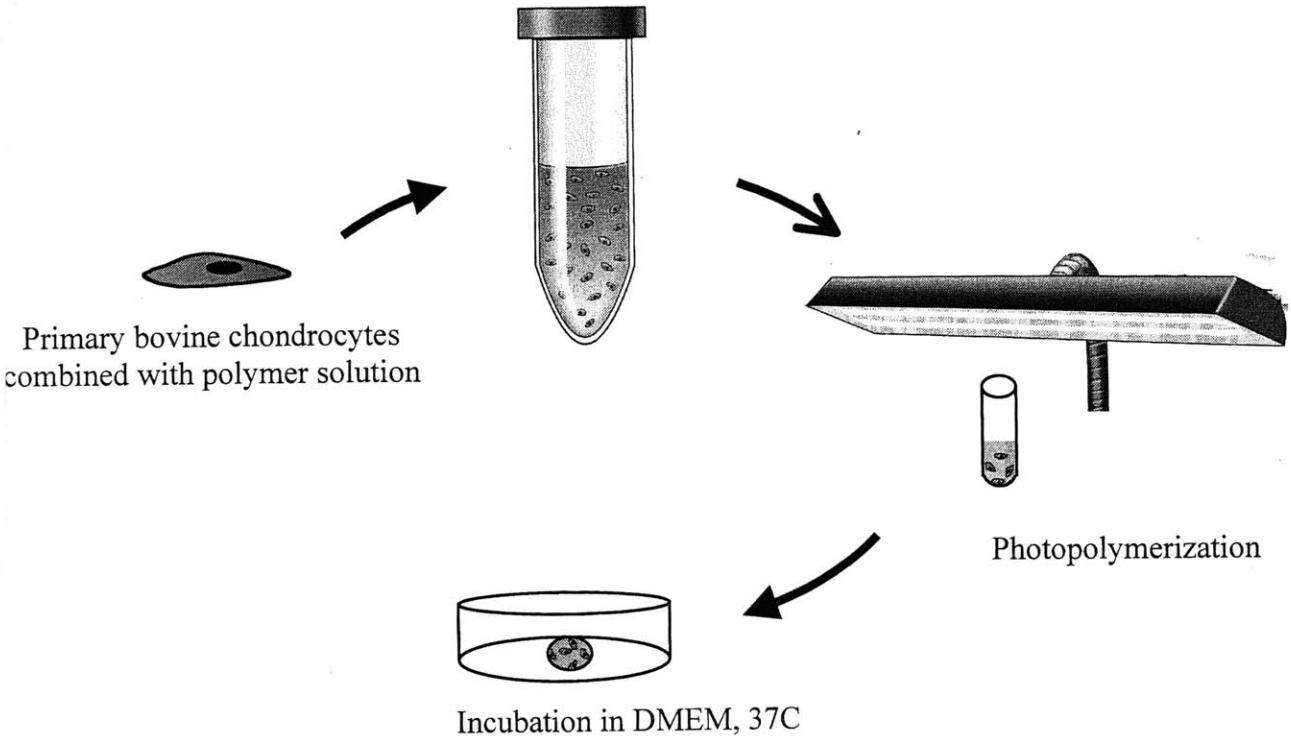

Figure 3.1. Experimental Protocol: Cells isolated from articular cartilage were mixed with poly(ethylene oxide)-dimethacrylate and poly(ethylene glycol) to a final concentration of 50 x 10^6 cell/cc. Aliquots of the cell/polymer suspension were then placed under 2 mW/cm^2 UVA light for 3 minutes and the resulting gels were incubated under static conditions.

3.4 Results

3.4.1 Cell Encapsulation. One day after photopolymerization, hydrogels grossly demonstrated a uniform distribution of viable cells stained by MTT (Fig. 3.2). Upon further examination by light microscopy a dispersion of cells within the hydrogel is observed (Fig. 3.3). Clusters of two to three cells are observed although most cells are individually dispersed. Heterogeneous chondrocyte morphology is observed with both ovoid and elongated cells present.

3.4.2 Construct Composition. Constructs exhibited increases in total collagen and GAG contents (% ww) from 3 to 14 days of static incubation (Fig. 3.4). The increases were statistically significant ($p<10^{-4}$). DNA content of the constructs decreased over the 14 days (Table 3.1, $p=0.043$). The polymer content of the control hydrogels declined during the first week of incubation and then remained constant. Hydrogel constructs with cells demonstrated a slower initial decrease in polymer content over the first week compared to controls but a subsequent increased rate of degradation. (Fig. 3.5).

3.4.3 Mechanical Analysis. Construct mechanical and electromechanical properties increased with time. Tissue engineered cartilage had significantly lower mechanical and electromechanical properties than natural cartilage, generally on the order of one magnitude below native cartilage (Fig. 3.6-8). The equilibrium modulus increased steadily from an initial (40% PEODM control) value of less than 1 kPa to over 70 kPa after 6 weeks of static incubation (Fig. 3.6). Control hydrogels synthesized using 100% PEODM have a higher static equilibrium moduli compared to 40% PEODM semiIPNs. The 100% and 40% PEODM gels show little difference in dynamic stiffness properties. The dynamic stiffness of the constructs increases to a large degree after only 3 weeks of

incubation compared to hydrogels and semiIPNs without cells (Fig. 3.7). A maximum dynamic stiffness in the engineered cartilage of 1 MPa is observed after 6 weeks incubation. The streaming potential of the constructs also increases with construct incubation (Fig. 3.8).

3.4.4 Histology. The tissue structure of the photopolymerized hydrogel constructs resembled cartilage (Fig. 3.9). The two-week constructs stained with H&E demonstrate ovoid and elongated cells surrounded by a basophilic extracellular matrix (Fig. 3.9a). A thin capsule (approximately one cell layer thick) is observed surrounding the cartilage-like tissue that forms the bulk of the construct (Fig. 3.9a). Cells are present in varying densities. Safranin-O clearly demonstrates the variation in cell distribution (Fig. 3.9b-d). Figure 3.9b and c shows a region of hypercellularity with cells surrounded by a matrix staining strongly for proteoglycans. Figure 3.9d demonstrates a region of the gel with both small clusters and individual cells. The pericellular region of individual cells and small clusters of cells stain for proteoglycans.

3.5 Discussion

Photopolymerization provides a fast, efficient method to convert a liquid to a gel *in situ* under ambient conditions.[13] Photopolymerization is used extensively in the dental community to form sealents on teeth and in caries.[14] Photopolymerization has also been used *in vivo* to form gels for the prevention of tissue adhesions.[15] This technique provides direct control of the polymerization process both temporally and spatially. For

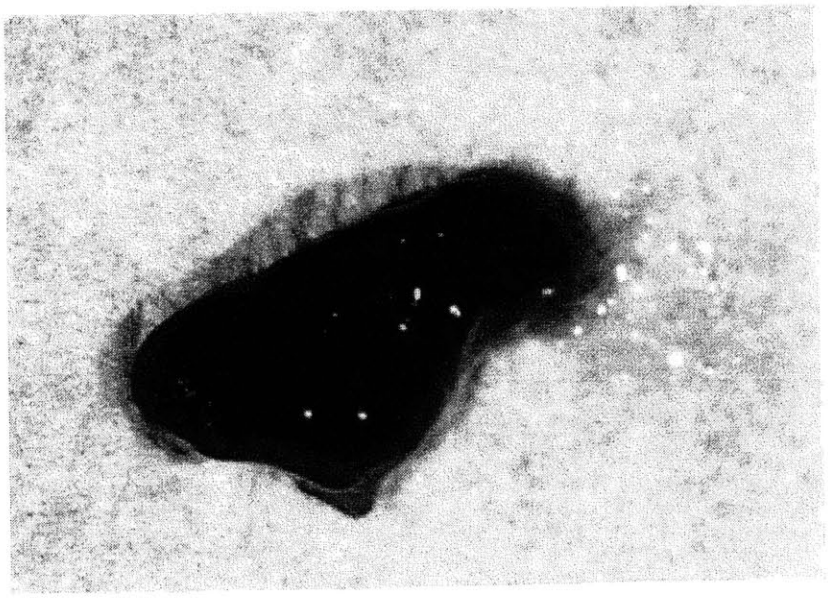

Figure 3.2. MTT staining of constructs one day after encapsulation demonstrate viable chondrocytes (4.5X).

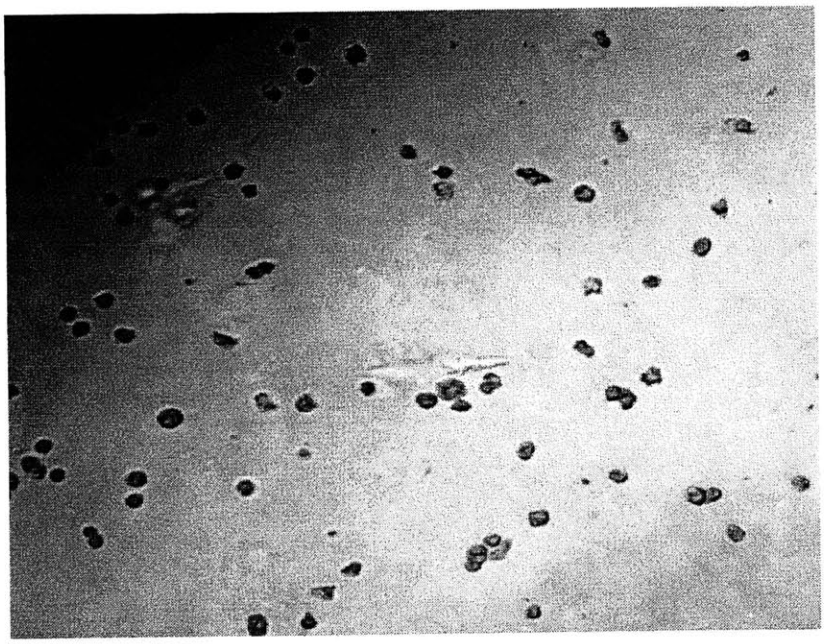

Figure 3.3. Light microscopy of cells dispersed in the gel with both ovoid and elongated morphology (100X).

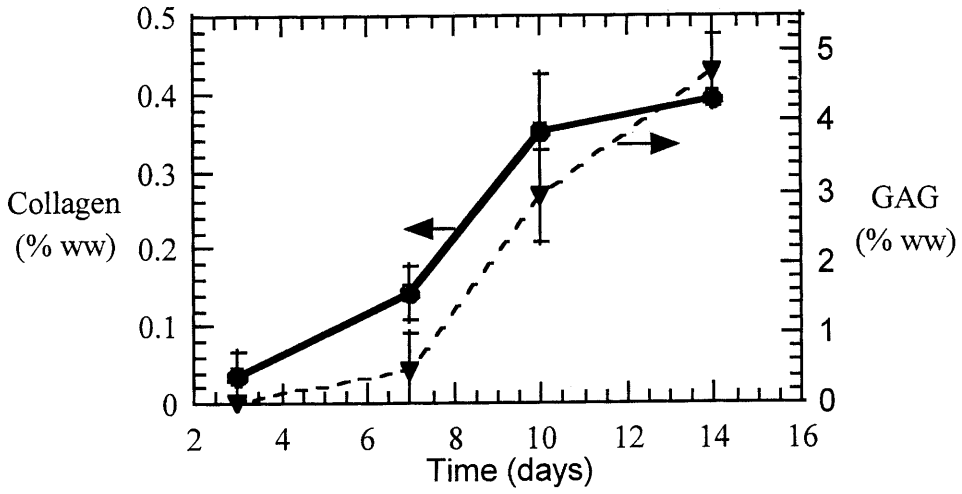

Figure 3.4. Biochemical analysis: GAG and total collagen contents of constructs (% wet weight).

Time (days)	Cell Content (Millions of Cells/mg)
3	0.041 ± 0.004
7	0.035 ± 0.006
10	0.032 ± 0.006
14	0.030 ± 0.007

Table 3.1. DNA content of constructs.

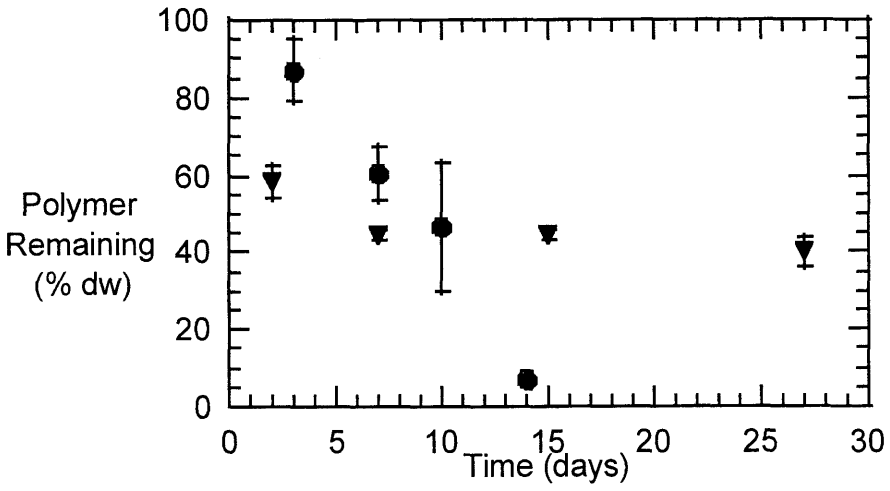

Figure 3.5. Polymer content (% dry weight) of control constructs without cells (--▲--) and cell constructs (--●--).

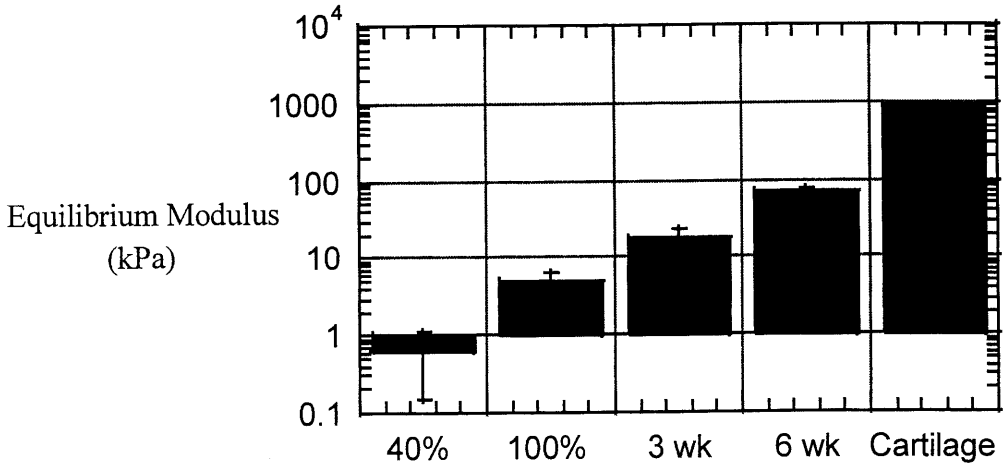

Figure 3.6. Equilibrium moduli of control PEODM hydrogels and ovine constructs after 3 and 6 weeks of incubation.

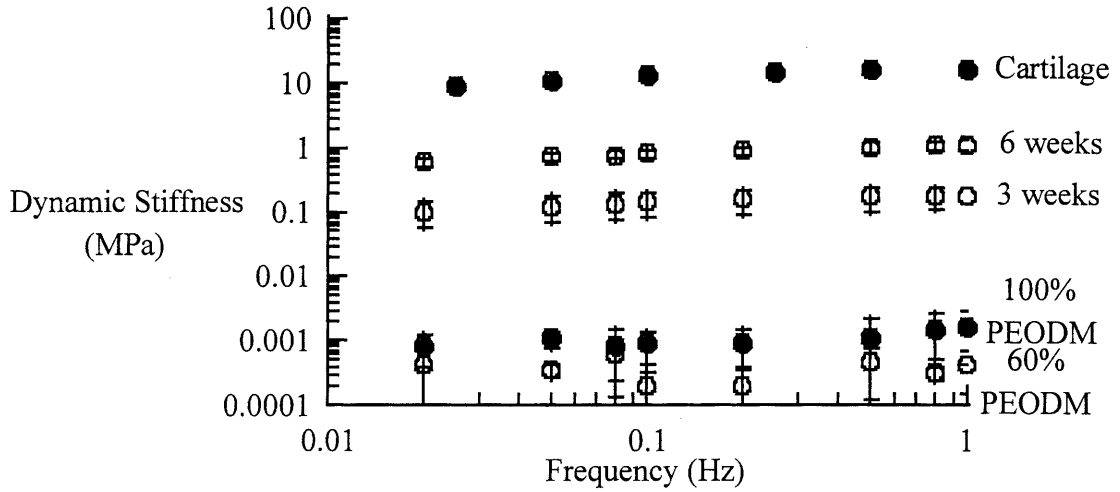

Figure 3.7. Dynamic stiffness of control PEODM hydrogels and ovine constructs after 3 and 6 weeks of incubation.

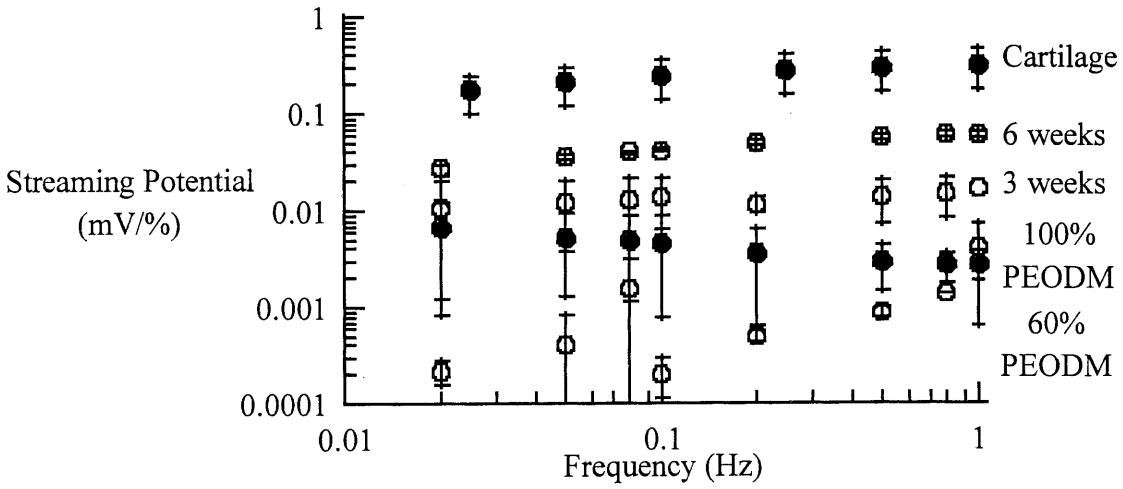

Figure 3.8. Streamin potential of control PEODM hydrogels and ovine constructs after 3 and 6 weeks of incubation.

A.)

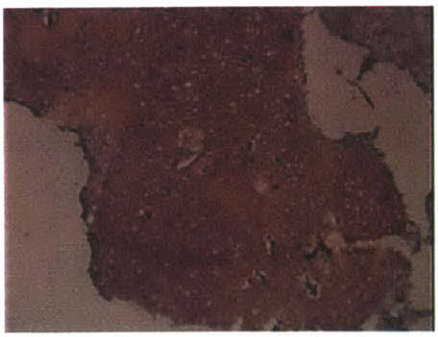

B.)

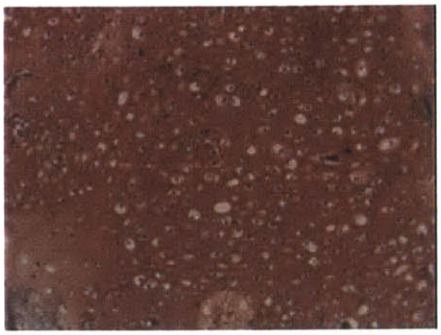

C.)

D.)

Figure 3.9. Histological cross-sections of hydrogel constructs after 2 weeks incubation stained with a.) hematoxylin and eosin, 100X, b.) safranin-O/fast green demonstrating proteoglycan distribution in a region of cartilage-like tissue, 100X, c.) 200X and d.) a region of sparsely distributed cells, 200X.

example, the reaction or gelation process proceeds only when and where light is exposed to the photopolymerizing polymer solution. Low concentrations of photoinitiator and UVA light which are cell compatible, yet still allow photopolymerization to proceed efficiently, can be used for cell photoencapsulation. The ability to encapsulate cells using a photopolymerization process would provide a method to efficiently distribute cells in a hydrogel system for tissue engineering or even drug delivery purposes.

High molecular weight poly(ethylene oxide) has been studied as an injectable scaffold for cartilage tissue engineering *in vivo*. While cartilage-like tissue formed after subcutaneous implantation in nude mice, the mechanical properties of the liquid polymer solution were lacking before tissue was able to form.[16] Additionally, since no gel is formed with PEO alone, *in vitro* study of the system is difficult. While *in* vivo studies are important for clinical applications, *in vitro* analysis of a tissue engineering system is desirable to avoid the influence and variability that animals add to a system.

Gels made from 40% PEODM were utilized for photoencapsulation of chondrocytes. Through the addition of PEODM to the PEO system, a covalently crosslinking network may be formed. 40% PEODM semiIPNs provide some mechanical strength with the covalent crosslinking, yet allow nutrient and waste transport and space for tissue development with the uncrosslinked PEO. This polymer combination was used as a model system for studying photoencapsulation of chondrocytes because of the biocompatibility of PEO with chondrocytes.[16] Other photoreactive polymers or polymer/initiator systems designed to influence cell movement or tissue formation could potentially be used.

Cartilage is composed of proteoglycans and collagen secreted by chondrocytes to form a functional, organized extracellular matrix. Chondrocytes react to both the biochemical and biomechanical signals provided *in vivo* to stimulate either matrix synthesis or degradation. While proteoglycan and collagen concentration and organization is heterogenous in native cartilage, measuring these matrix components provides information regarding the proclivity of the chondrocytes to form cartilage-like tissue within a particular scaffold or encapsulation system.

The concentration of both proteoglycans and collagen increased with incubation time. Early time points (3, 7, 10 and 14 days) were studied in order to learn the initial matrix production capabilities of the gel/chondrocyte constructs. Initial matrix deposition is crucial to the survival and functionality of the constructs both *in vitro* where scaffolds may be degrading and providing less support and *in vivo* where harsh mechanical forces are present. The biochemical results show that the chondrocytes survive the encapsulation process and that the gel scaffold allows for efficient chondrocyte matrix production during the two weeks studied. While the GAG contents were similar to native cartilage the collagen content was well below normal and other tissue engineered cartilage. It may be hypothesized that with longer incubation times further matrix will be produced and secreted. PGA scaffolds incubated *in vitro* showed continual increased matrix production and organization for over 6 months of *in vitro* incubation.[3] If the photopolymerizing gel system was injected *in vivo*, the presence of biochemical and mechanical signals for matrix production may further enhance matrix production and organization.

The decrease in cell content observed in the first week of incubation may come from a variety of sources. First, the cells were isolated from bovine femoropatellar cartilage and used immediately. The stress of enzymatic isolation may be responsible for some decrease in cell content. Second, the gel erodes during the first of incubation. Little extracellular matrix has been deposited at this time so the cells may diffuse from the construct along with the polymer.

The histology sections of the two-week hydrogels constructs also demonstrate extracellular matrix production along with interesting morphological features (Fig. 3.9). The safranin-O/fast green staining shows clearly large regions of cartilage-like tissue, which appears to be hypercellular and secreting large amounts of proteoglycans. On the other hand, there are also some regions that have small clusters and individual cells staining for proteoglycans. The sparsely distributed cells appear viable and are secreting matrix. Eventually, these clusters and individual cells may continue to grow and coalesce to form a uniform matrix with further incubation. The high viscosity of the polymer solution before gelation or the gelation process itself may be responsible for the variations in cell density in the gel constructs.

Semi-interpenetrating networks, semiIPN, are comprised of both covalently crosslinked PEODM and PEO physically entrapped within the PEODM gel. The PEO can diffuse from semiIPN allowing space for extracellular matrix deposition or tissue formation. While the PEO is able to diffuse from the hydrogels, the PEODM must be degraded. Increasing the PEODM content of the semiIPN increases the crosslinking density or mechanical strength of the gel. The increase in crosslinking density may be observed in both the decreased swelling of the hydrogels previously determined and the

biomechanical properties found in this study (Fig. 3.6-8).[17] The degradation of the hydrogels was altered in the presence of the chondrocytes (Fig.3.5). Chondrocytes produce esterases and other enzymes that may be responsible for the enhanced hydrogel degradation. Complete degradation of the polymer is desirable for tissue engineering cartilage so that only the desired tissue, in this case cartilage, is present.

The mechanical properties of tissue engineered constructs provides valuable information on the functional and matrix properties of the tissue. Thus, biomechanical data further aids in determining the tissue engineering potential of a scaffold system. It has been demonstrated that the concentrations of GAG, collagen and water in cartilage are related to the physical properties of the tissue. For example, it has been reported that the equilibrium modulus increases with increasing GAG and decreasing water content.[18] The dynamic stiffness and streaming potential provide information regarding the total matrix deposition and quality.[18] The increase in dynamic stiffness and streaming potential with frequency is caused by the increasing fluid velocity in the constructs as higher compression rates are applied.[8] In the case of dynamic stiffness, the observed increase with time is due to the increased frictional interaction between the interstitial fluid and matrix. The streaming potential is caused by the flow of fluid past immobilized fixed charge. The majority of fixed charge (at physiological pH) is found on GAG. The increasing streaming potential implies that GAG is being functionally immobilized into a matrix in the gels.[8] The increase in the equilibrium modulus, dynamic stiffness and streaming potential with time suggests that the encapsulated chondrocytes synthesized functional extracellular matrix (Fig. 3.6-8).

3.6 References

1. Langer, R. & Vacanti, J., Tissue Engineering. *Science* **260**, 920-926 (1993).

2. Mow, V.C., Radcliffe, A. & Poole, A.R., Review: Cartilage and diarthrodial joints as paradigms for hierarchical materials and structures. *Biomaterials* **13**, 67-97 (1992).

3. Freed, L., *et al.*, Biodegradable Polymer Scaffolds for Tissue Engineering. *Bio/technology* **12** (1994).

4. Paige, K.T., Cima, L.G., Yaremchuk, M.J., Vacanti, J.P. & Vacanti, C.A., Injectable Cartilage. *Plastic and Reconstructive Surgery* **96**, 1390-1400 (1995).

5. Guo, J., Jourdian, G. & MacCallum, D., Culture and Growth Characteristics of Chondrocytes Encapsulated in Alginate Beads. *Connectice Tissue Research* **19**, 277-297 (1989).

6. Paige, K., *et al.*, De Novo Cartilage Generation Using Calcium Alginate-Chondrocyte Constructs. *Plastic and Reconstructive Surgery* **97**, 168-178 (1996).

7. Atala, A., *et al.*, Injectable alginate seeded with chondrocytes as a potential treatment for vesicoureteral reflux. *Journal of Urology* **150**, 745-747 (1993).

8. Buschmann, M.D., Gluzband, Y.A., Grodzinsky, A.J., Kimaru, J.H. & Hunziker, E.B., Chondrocytes in Agarose Culture Synthesize a Mechanically Functional Matrix. *Journal of Orthopedic Research* **10**, 745-758 (1992).

9. Silverman, R., Passaretti, D., Huang, W., Randolph, M. & Yaremchuk, M., Injectable tissue engineered cartilage using a fibrin glue polymer. *Plastic and Reconstructive Surgery* **in press**.

10. Farndale, R., Buttle, D. & Barrett, A., Improved quantitation and discrimination of sulphated glycosaminoglycans by the use of dimethylmethylene blue. *Biochim Biophys Acta* **883**, 173-177 (1986).

11. Woessner, J.F., The determination of hydroxyproline in tissue and protein samples containing small proportions of this imino acid. *Archiv. Biochem. & Biophys.* **93**, 440-447 (1961).

12. Kim, Y., Sah, R., Doong, J. & al, e., Fluorometric assay of DNA in cartilage explants using Hoechst 33258. *Anal Biochem* **174**, 168 (1988).

13. Decker, C., UV-Curing Chemistry: Past, Present and Future. *Journal of Coatings Technology* **59**, 97-106 (1987).

14. Venhoven, B.A.M., de Gee, A.J. & Davidson, C.L., Light initiation of dental resins: dynamics and polymerization. *Biomaterials* , 2313-2318 (1996).

15. Hill-West, J., *et al.*, Prevention of postoperative adhesions in the rat by in situ photopolymerization of bioresorbable hydrogel barriers. *Obstet Gynecol* **83**, 59-64 (1994).

16. Sims, D., *et al.*, Injectable Cartilage Using Polyethylene Oxide Polymer Substrates. *Plastic and Reconstructive Surgery* **98**, 843-850 (1996).

17. Elisseeff, J.H., *et al.*, Transdermal Photopolymerization of PEO-based Injectable Hydrogels for Tissue Engineering Cartilage. *Plastic and Reconstructive Surgery* **in press** (1998).

18. Frank, E.H. & Grodzinsky, A.J., Cartilage Electromechanics-I. Electrokinetic transduction and the effects of electrolyte pH and Ionic Strength. *J. Biomechanics* **20**, 615-627 (1987).

Chapter 4. *In vivo* Transdermal Photopolymerization of Chondrocytes in PEO-based Hydrogels.*

4.1 Introduction

The previous chapter demonstrated the ability to encapsulate chondrocytes in a photopolymerizing hydrogel *in vitro*. The encapsulated cells produced a functional matrix suggesting their potential use of the photopolymerization system for tissue engineering cartilage. The next step in studying the efficacy of transdermal photopolymerization for clinical cartilage replacement is *in vivo* study. This chapter addresses the tissue engineering of cartilage in athymic (nude) mice for up to 7 weeks.

4.2 Background

Reconstructive, orthopedic and plastic surgeons are continually faced with the challenge of replacing cartilage lost by trauma, arthritis, or congenital abnormalities.[1] Due to limitations in the self-repair capability of cartilage, current therapies for cartilage replacement include allogenic and alloplastic implants. These methods suffer from many problems including lack of donor tissue availability, rejection, increased susceptibility to infection and toxicity.[2] Tissue engineering cartilage provides a method to replace lost tissue with normal functional tissue. Tissue engineering of cartilage could potentially provide a method to replace cartilage function in articular joints for orthopedic applications and cartilage structure in plastic surgery.

---

* This chapter is in press for publication in *Plastic and Reconstructive Surgery*

Tissue engineering has been defined as "the use of living cells, together with extracellular components (natural or cellular) in the development of implantable parts or devices for the replacement or restoration of function".[3] Specifically, cartilage has been tissue engineered both *in vitro* and *in vivo* using a variety of biocompatible polymers including poly(glycolic acid), (PGA).[1] PGA scaffolds have been seeded with chondrocytes, incubated in bioreactors and then implanted subcutaneously in nude mice or intra-articularly in rabbits.[2, 4]

Recently, new methods for minimally invasive injection of chondrocytes and chondrocyte/polymer suspensions have been investigated. The injection of isolated chondrocytes has been shown to promote cartilage repair.[5] *In vivo* injection of both a scaffold and cells has been performed using calcium alginate, fibrin glue, and poly(ethylene oxide), PEO as described in Chapter 4.[6, 7] In contrast to injecting cells alone, a scaffold provides a three-dimensional matrix on which the chondrocytes can proliferate, produce matrix and form functional tissue in a desired shape.[8] The scaffold may also provide mechanical stability for developing cartilage, particularly in joints which are subjected to large forces.

An injectable gel system provides a method to non-invasively implant a polymer/cell construct for cartilage tissue engineering. Noninvasive implantation of cartilage would be highly advantageous for both orthopedic and plastic surgery applications. For example, an injectable cartilage replacement system in the joint would prevent the need for open surgery, requiring only orthoscopic surgery for implantation. Similarly, for plastic surgery applications simply a needle injection and transdermal

photopolymerization may be required as opposed to an incision. [5] The ability to transdermally photopolymerize, or photopolymerize polymer and cells through the skin, has been studied *in vivo* for applications in minimally invasive implantation and craniofacial cartilage replacement.[5]

Previously, viscous solutions of PEO and chondrocytes injected subcutaneously in nude mice formed neocartilage.[7] While these results proved the efficacy of PEO in supporting cartilage formation, the linear PEO chains diffused away rapidly and lacked structural and mechanical integrity. Thus, to address these issues, we have utilized PEO together with substituted PEO and photopolymerization to create a light-sensitive gelation process that yields PEO scaffolds with improved structural integrity. Photoinduced gelation provides spatial and temporal control during scaffold formation, permitting shape manipulation after injection and during gelation *in vivo*. In addition to designing a photoreactive scaffold for cartilage replacement, a minimally invasive, transdermal photopolymerization technique was employed to implant the scaffolds, allowing simply exposure of the skin surface to light in order to induce gelation of scaffolds injected subcutaneously (Figure 4.1).[9]

4.3 Methods

4.3.1 *Chondrocyte Isolation*. Saddle sections from 2-4 week old bovine calves were obtained from a local abattoir within 8 hours of slaughter. Articular cartilage from the bovine femoropatellar groove was dissected and cut into small chunks and digested in collagenase (0.2%) for 14-16 hours and poured through a nytex filter to isolate cells. The cell suspension was centrifuged and washed with phosphate buffered saline (PBS) three

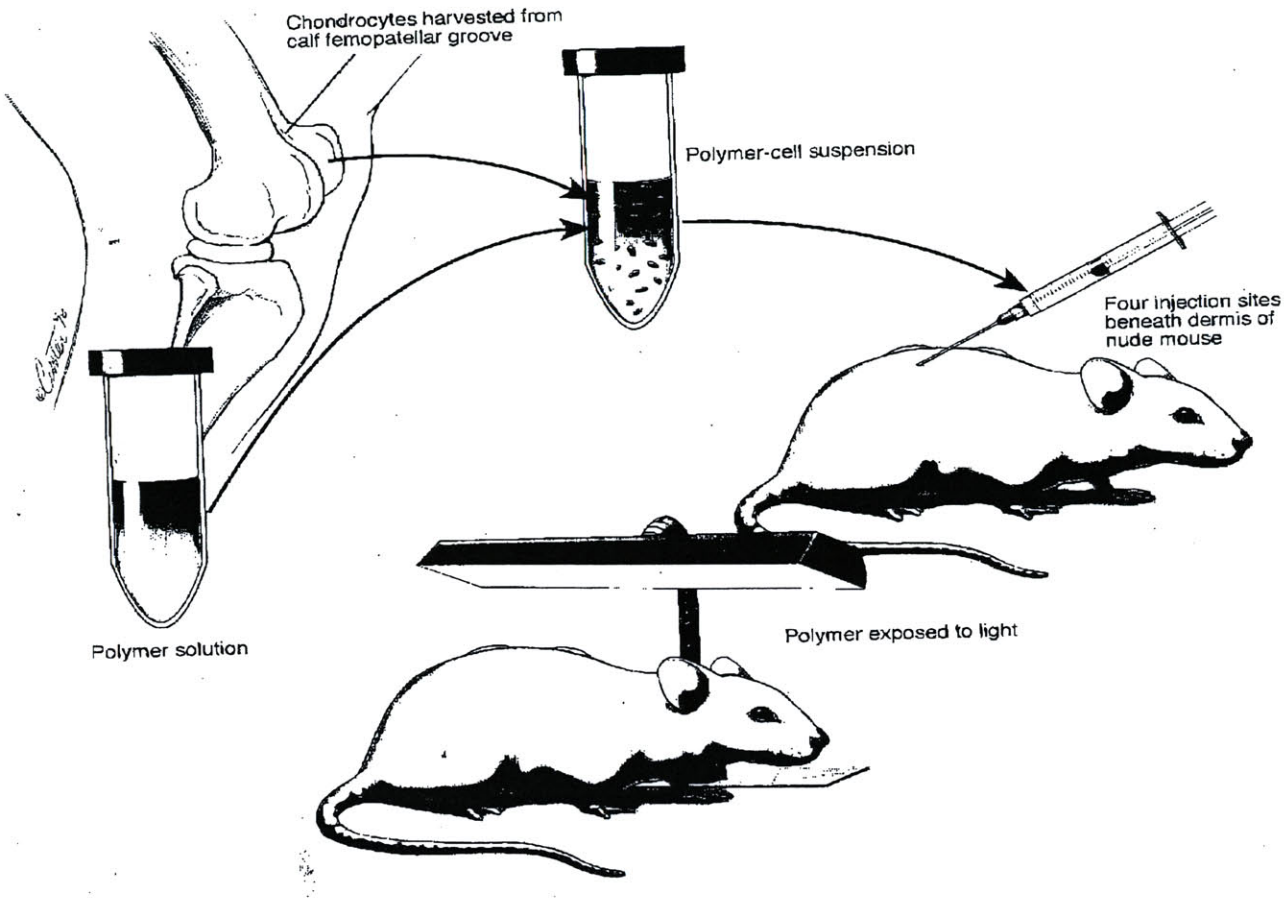

Figure 4.1. Schematic of procedure for cartilage tissue engineering using transdermal photopolymerization depicting i.) isolation of bovine chondrocytes from the femoropatellar groove and combination with polymer (10-20% PEODM) to form ii.) a polymer/ chondrocyte suspension. The polymer/chondrocyte suspension is subsequently iii.) injected subcutaneously on the dorsal surface of a nude mouse and iv.) photo-polymerized by placement of the mouse under an UVA lamp 3 minutes.

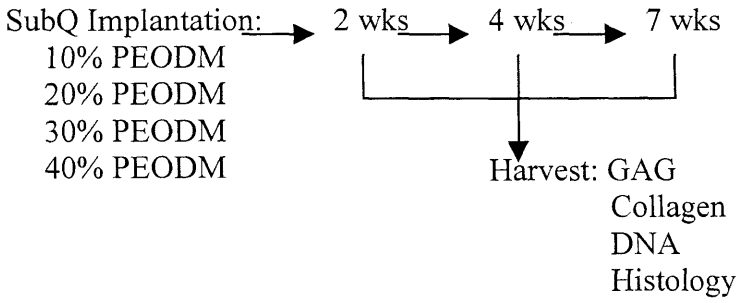

Figure 4.2. Experimental Protocol.

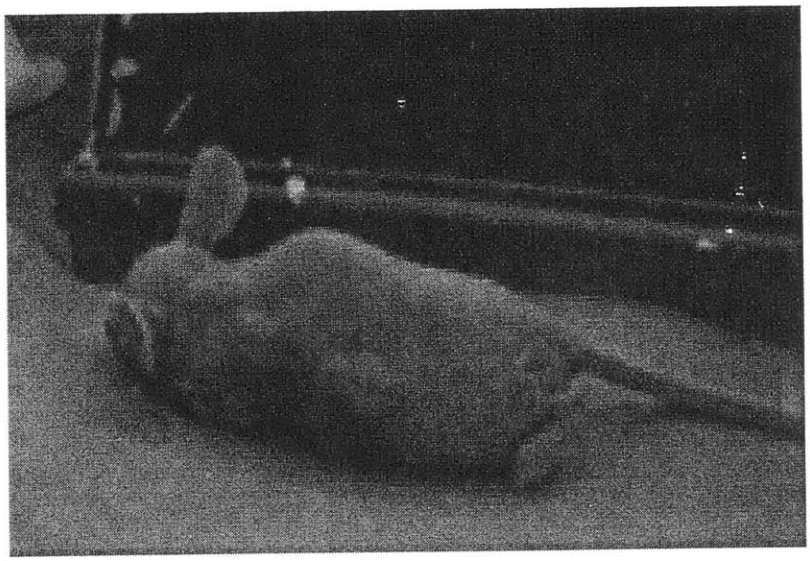

Figure 4.3. Athymic mouse undergoing transdermal photopolymerization under a low intensity UVA lamp.

Figure 4.4. Hydrogel implant post-photopolymerization.

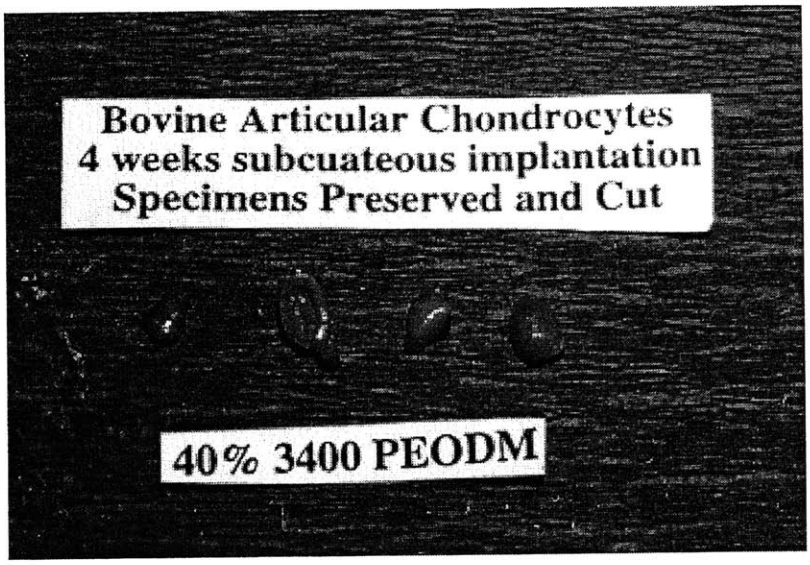

Figure 4.5. 40% PEODM tissue-engineered constructs harvested after 7 weeks implantation in a nude mouse.

times. The primary chondrocytes were counted with a hemocytometer and added to a polymer and PBS suspension to a final concentration of 50 million cells/cc.

4.3.2 *Polymer Preparation.* Poly(ethylene oxide)-dimethacrylate, PEODM, MW 3400 (Shearwater Polymers) and PEO MW100K were dissolved in PBS to make a 20% (w/w) solution. The relative concentration of crosslinking polymer (PEODM) to linear polymer (PEO) studied was 10:90 (10% PEODM), 20:80, 30:70, and 40:60 (40% PEODM) PEODM:PEO. The photoinitiator, 1-hydroxycylcohexyl phenyl ketone (HPK, Polysciences), was added to make a final concentration of 0.01% (w/w). The equilibrium swelling constant of the hydrogels was determined using the following equation:

$$Q = \frac{vs + vp}{vp}$$

where v_p is the volume of the polymer and v_s is the volume of solvent (water) present within the hydrogel when swollen. Hydrogels were formed after exposure of 10-40% PEODM/PEO polymer solutions (150 μl aliquots each) to UVA light for 4 minutes. The resulting semi-interpenetrating networks (semiIPNS) consisted of both crosslinked and uncrosslinked PEO. Gels were swollen in PBS for 3 hours to determine the water content. The gels were lyophilized to obtain the dry weight and subsequent volume of polymer.

4.3.3 *Implantation and Harvest.* Twelve athymic female mice (Charles River Laboratories, Massachusetts General Hospital) were anesthetized with methoxyfluorane and injected with polymer/chondrocyte suspension. Each mouse received one aliquot (0.12 ml) from each of the four polymer compositions (10, 20, 30, 40% PEODM). Control mice comprised of injections of polymer alone (40% PEODM). Following

injection mice were placed 2 inches below a UVA lamp (GloMark Systems) to permit exposure to an intensity of 2 mW/cm^2 for 3 minutes as measured by radiometer. The polymer/chondrocyte hydrogel was palpated to observe the progression of polymerization. Four mice were sacrificed at 2, 4 and 7 weeks by pentobarbitol overdose. To determine the relative amounts of collagen type I and type II formed in the constructs, seven additional mice were injected with four 0.1 ml aliquots of 35% PEODM and 50 million cells/cc and photopolymerized as described above. The mice were sacrificed after 6 weeks (7 mice, 28 constructs). All constructs were carefully removed and weighed to obtain the implant wet weight.

4.3.4 *Construct Analysis.* Constructs were dried under vacuum for at least 24 hours after which dry weights were obtained. The dried constructs were subsequently digested by addition of 1 ml of papain solution (125 μg/ml Papain, 100mM phosphate buffer, 10mM cysteine, 10mM EDTA, pH 6.3) and incubated in a water bath at 60°C for 16 hours. The concentration of chondroitin sulfate was determined using the DMMB dye assay as previously described.[10] Total collagen content was determined by hydroxyproline content, as previously described.[11] The DNA content of the constructs was determined by the Hoechst dye method and cell number was calculated using the conversion factor of 7.7 pg DNA/chondrocyte.[12] Results are given as average and standard deviation (n=4). Statistical analysis was performed using Minitab Software. Time and % PEODM were the two factors studied using a randomized complete block design and ANOVA analysis.

The ratio of collagen type I and II was determined for 35% PEODM constructs and three bovine articular cartilage control samples.[13] Constructs for collagen analysis were

digested in formic acid (70%) for 1 hour at 60°C followed by overnight incubation at room temperature in CNBr (0.55 g/ml) in formic acid. After drying, the samples were redissolved in reducing sample buffer (Owl Separation Systems) and incubated at 80°C for 10 minutes. Approximately 50 μg of digested collagen was added to each lane in a 15% polyacrylamide gel. The gel was run at 100 V for 1.5 hours, stained with Coomassie blue for 45 minutes and destained overnight. The ratio of CB10 and CB11 collagen peptide fragments were analyzed using NIH Image.[13]

4.4 Results

4.4.1 Polymer. The equilibrium swelling constant, or equilibrium swelling volume ratio, of the PEODM/PEO semi-IPNs are given in Table 4.1 along with gross observations of the gels. The 10 and 20% PEODM networks dissolved completely in PBS therefore no swelling could be observed. The 30% and 40% PEODM networks exhibited an equilibrium swelling volume of 16.89 and 16.02 respectively, both increased compared to 100% PEODM networks which had an equilibrium swelling constant of 9.81.

4.4.2 Biochemistry. The biochemical composition of the neocartilage formed was analyzed as a function of polymer matrix composition (10, 20, 30 and 40% PEODM) and time (2, 4, and 7 weeks). Harvested implants (40% PEODM, one-month implantation) are shown in Figure 4.5. Grossly, constructs are avascular and opaque, characteristics of native cartilage. Biochemical results are described in Figures 4.6 and 4.7. The glycosaminoglycan, GAG, contents at 7 weeks ranged from 2.8% per construct wet weight in the 10% PEODM hydrogels to 1.5% per wet wt. in the 40% PEODM hydrogels (Figure 4.6). GAG content decreased with increasing % PEODM ($p<10^{-4}$, Table 4.3).

% PEODM	Equilibrium Swelling Constant Q	Gross Observations
10	dissolved	-
20	dissolved	-
30	16.89 ± 4.72	opaque/white
40	16.02 ± 1.27	opaque/white
100	9.81 ± 0.58	clear

* Values are average ± standard deviation (n=4)

Table 4.1. Equilibrium swelling constants and physical characteristics observed in semi-interpenetrating networks/gels of varying % PEODM.

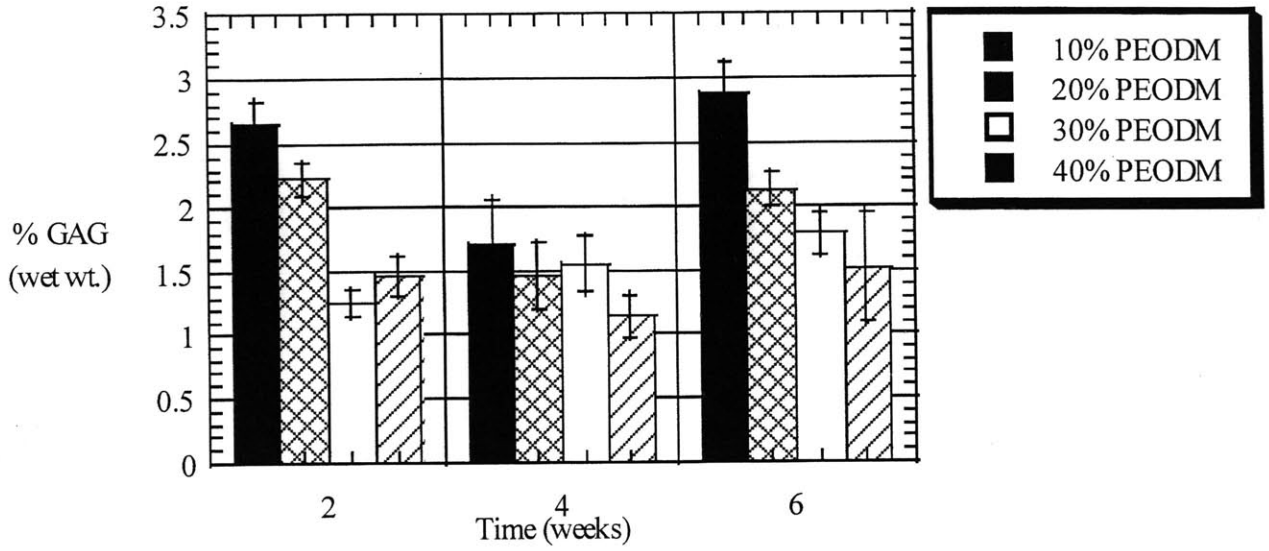

Figure 4.6. The percentage of GAG per construct wet weight over time in hydrogels of varying PEODM concentration.

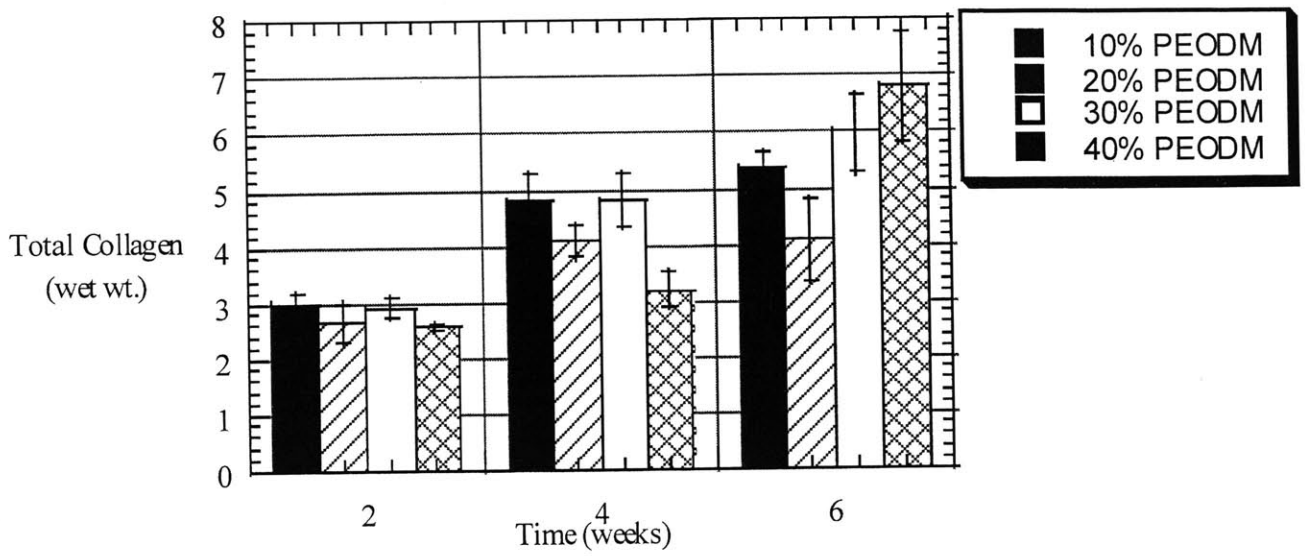

Figure 4.7. The percentage of collagen per construct wet weight over time in hydrogels of varying PEODM concentration.

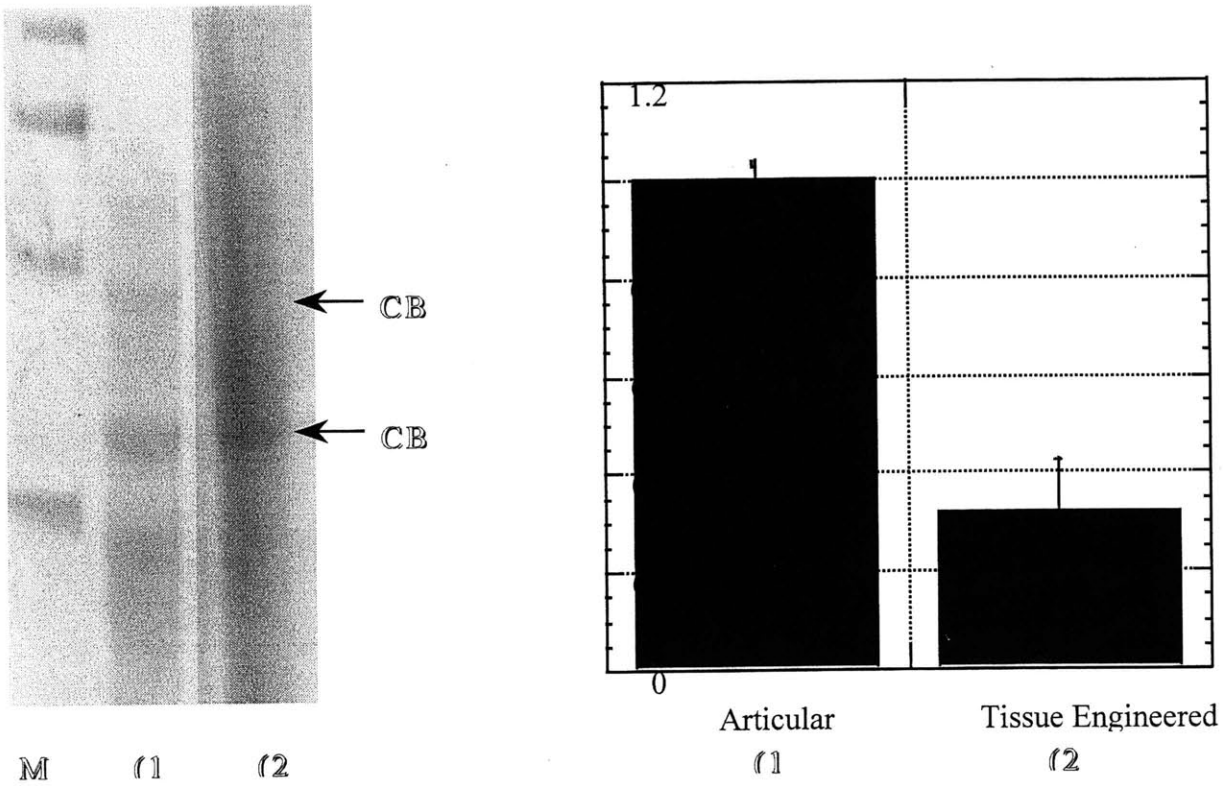

Figure 4.8. SDS-PAGE gel to determine the Collagen II/I ratio in 35% PEODM constructs harvested after 6 weeks and control bovine articular cartilage.

	DNA Content (millions of cells/mg wet weigl		
% PEODM	2 weeks	4 weeks	7 weeks
10	0.021 ± 0.0021	0.034 ± 0.015	0.02 ± 0.0024
20	0.018 ± 0.0018	0.016 ± .0063	0.018 ± 0.0063
30	0.037 ± 0.0042	0.025 ± 0.0075	0.015 ± 0.016
40	0.028 ± 0.0019	0.016 ± 0.0027	0.023 ± 0.0041

Table 4.2. DNA content of hydrogels with varying % PEODM at 2, 4 and 7 weeks.

Factor		SS	MS	F	p
Time	GAG	2.99	1.49	7.01	0.003
	Collagen	53.47	25.74	40.66	$<10^{-4}$
	DNA	3.15×10^{-4}	1.58×10^{-4}	1.06	0.36
% PEODM	GAG	7.6	2.53	11.88	$<10^{-4}$
	Collagen	5.26	1.75	2.66	0.067
	DNA	2.07×10^{-4}	6.88×10^{-5}	0.46	0.71

Table 4.3. Statistical analysis of biochemical data. SS = Sum of Squares, MS = Mean of Squares, F = Variance Ratio used to determine the probability (P) from a Fischer Table.

The total collagen content of the 10% PEODM hydrogel was 5% per wet weight at 7 weeks while the 40% PEODM constructs contained 6.5% per wet weight at 7 weeks with no statistically significant difference among the various % PEODM observed (Figure 4.7, Table 4.3). Both the total collagen and GAG contents increased with time. In addition there was a statistically significant interaction between time and % PEODM for collagen. As time increased the difference among PEODM groups also increased with 40% PEODM having the largest total collagen value. The DNA contents (millions of cells per mg wet weight) remained constant with time and polymer composition (Tables 4.2 and 4.3). The percent of Type II collagen present after 6 weeks of subcutaneous implantation was 35% ($\pm$ 11) (Figure 4.8).

4.4.3 Histology. Safranin O stained tissue sections of the 10, 20, 30 and 40% PEODM constructs demonstrated a distribution of GAG, a product of differentiated chondrocytes, throughout the constructs (7 weeks, Figure 4.9a-d). The tissue structure is characteristic of cartilage including ovoid shaped cells surrounded by an extracellular matrix. Mitotically active cells are observed in all tissue sections. Control constructs of polymer without chondrocytes were acellular with a thin, fibrous capsule surrounding the implant (H&E staining, not shown).

4.5 Discussion

Photopolymerization is a technique used frequently in dentistry to form sealants and dental restorations *in situ.*[14] Photopolymerization has been utilized to form hydrogels for preventing post-surgical adhesions and restenosis after angioplasty.[15, 16] From a tissue engineering implantation perspective, photopolymerization provides a fast

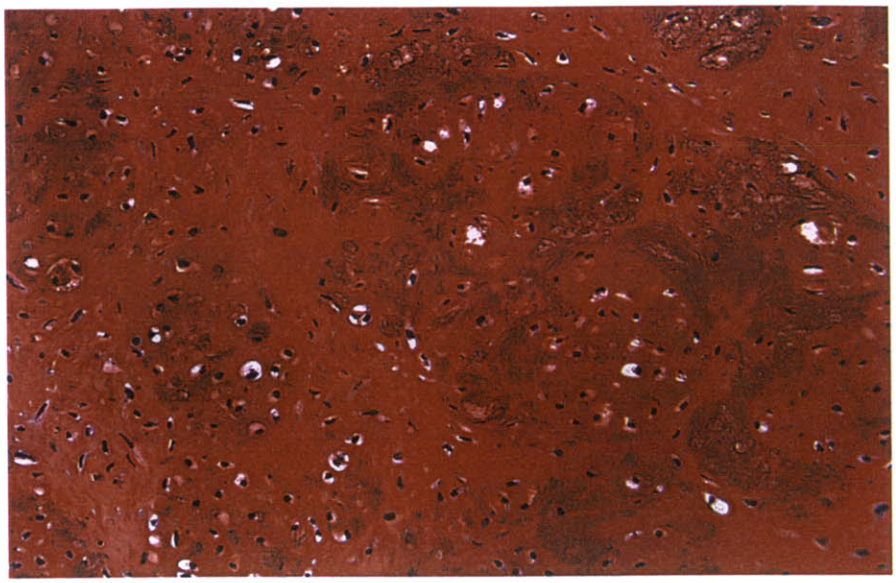

a.)

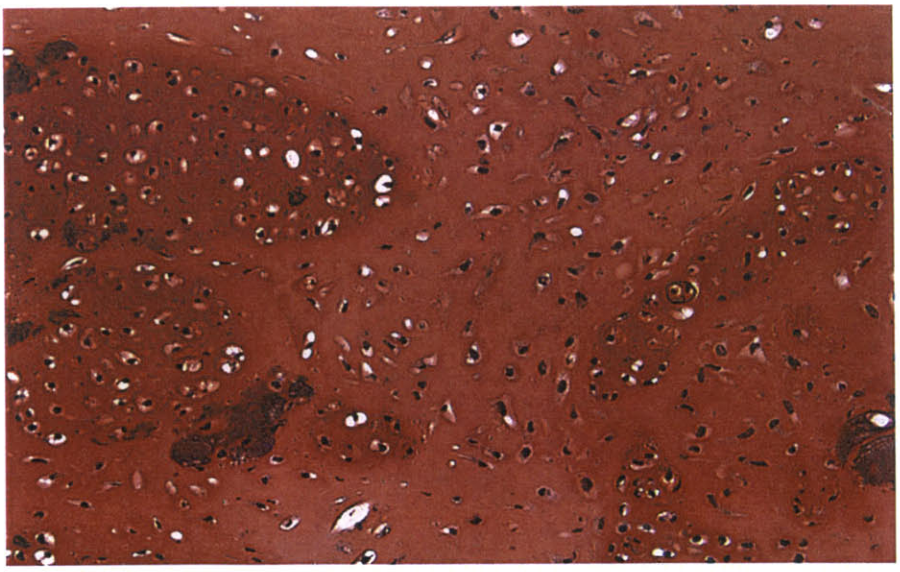

b.)

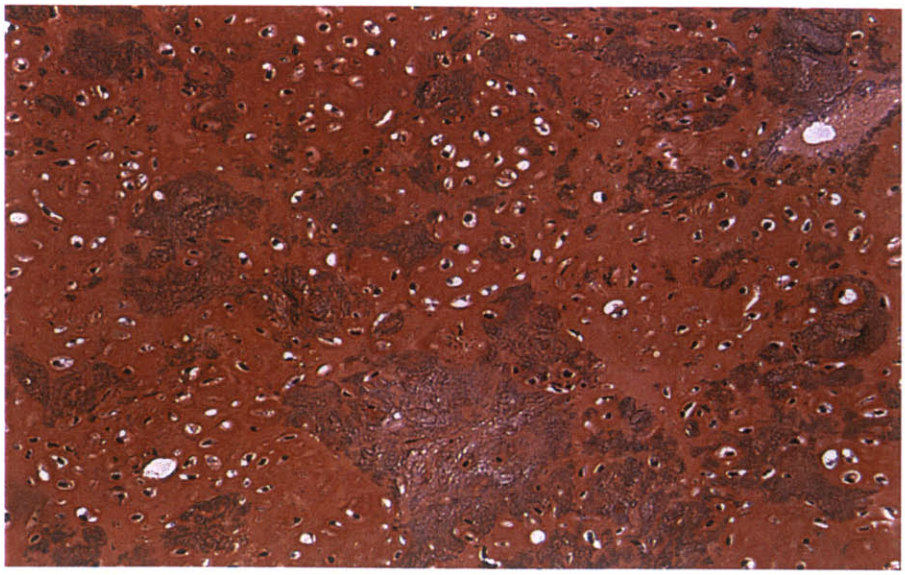

c.)

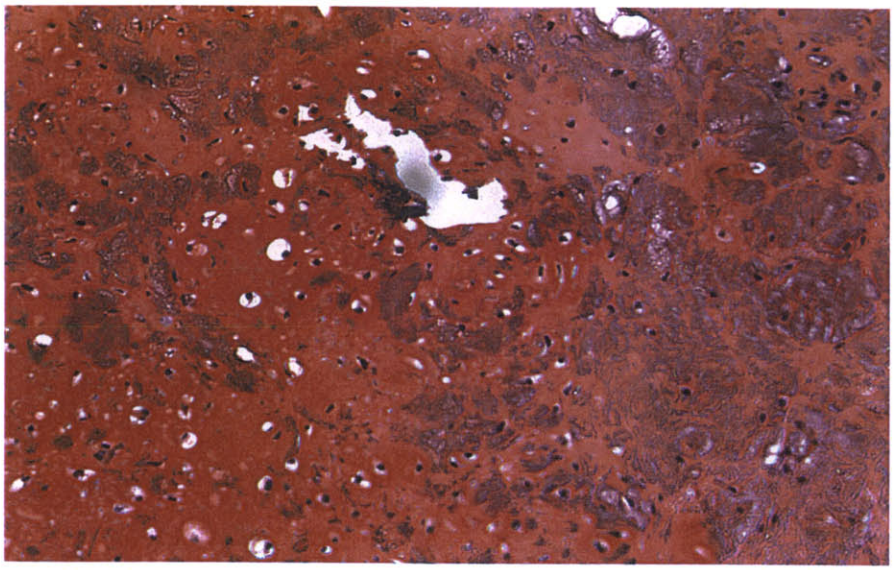

d.)

Figure 4.9. Safranin O stained histological sections of a.) 10%, b.) 20%, c.) 30% and d.) 40% PEODM constructs harvested after 7 weeks (200 X).

and efficient method to form a solid hydrogel from a liquid polymer solution *in vivo*. Transdermal photopolymerization provides physicians with a method to inject and mold synthetic implants and create autologous cartilage through tissue engineering in a minimally invasive manner.

In this study, PEO endcapped with methacrylate groups, PEODM, was utilized as a photocrosslinkable macromer. Radicals produced by a photoinitiator react with the methacrylate groups to cause polymerization leading to hydrogel formation or conversion of the liquid polymer solution to a solid network. A wide range of wavelengths of light can be used to cause a photopolymerization. By addition of an appropriate photoinitiator, visible light or UVA light can used to photopolymerize a polymer. UVB light has limited tissue penetration and may potentially damage tissue. UVA light was chosen for transdermal photopolymerization due to the high efficiency of UVA photoinitiators, allowing hydrogel formation beneath tissue to occur faster and with less intense light.

Light is attenuated by skin. Thus, the depth of implantation plays a critical role in determining the exposure time required to cause hydrogel formation as described in Chapter 2.[17] Increasing the depth of implantation, or the thickness of skin that the light must penetrate, increases the time of light exposure and the intensity of light required to photopolymerize the polymer. The light intensity and exposure time necessary to transdermally photopolymerize an implant under varying thickness of skin were modeled in Chapter 2.[17] Only three minutes of exposure to 2 mW/cm^2 UVA light, an intensity comparable to commercial tanning bed lamps, is required to convert a liquid PEODM polymer solution to a solid hydrogel subcutaneously in the mice used in this study. The

experimental technique of polymer/cell injection and photopolymerization is shown in Figure 4.1.

Photopolymerization or hydrogel formation may be controlled by the duration, intensity, and time of exposure of the polymer to light. For example, spatial resolution may be accomplished by simply exposing part of the liquid polymer to light. Temporal control may be attained by simply removing or supplying the light source. Finally, the ability to cause a photopolymerization through the skin provides a minimally invasive technique to implant hydrogel constructs by simply injecting a viscous, photocurable solution through a needle. Figures 4.3 and 4.4 demonstrate an athymic mouse during transdermal photopolymerization and the resulting implants.

The objective of this study was to determine if chondrocytes could survive injection and photopolymerization in PEO-based hydrogels and form tissue including an extracellular matrix comparable to natural cartilage. In particular, the effect of increasing the crosslinking density (i.e., increasing PEODM content) on cartilage formation was studied (see experimental protocol, Figure 4.2). The PEODM is the crosslinking macromer and thereby controls the crosslinking density and mechanical properties of the final gel. The PEO serves to increase the viscosity of the solution to facilitate injection and help maintain an open pore structure for cell encapsulation. Thus, the content of PEODM in the hydrogels plays an important role in the water content and mechanical integrity of the resulting semi-IPN that is formed while the PEO serves to aid nutrient and waste transport. The 10 and 20% PEODM semi-IPNS exhibit little resistance to palpation when injected subcutaneously and photopolymerized, similar to solutions of pure, uncrosslinked PEO. The 30% network begins to show maintenance of structure upon

palpation, while the 40% PEODM shows good resistance to compression upon palpation after polymerization. These gross *in vivo* observations were confirmed by equilibrium swelling volumes that were determined *in vitro*. The equilibrium swelling volume, Q, is a function of the water content of the network and provides information regarding the crosslinking density and mechanical properties.[18] The 10 and 20% networks dissolved completely in PBS, therefore swelling could not be observed. The 30 and 40% networks exhibited increasing equilibrium swelling (larger pore size and higher water content) than 100% PEODM hydrogels (Table 4.1).

The nude mouse model has been used extensively in the field of tissue engineering to study the potential of new biomaterials *in vivo*.[7, 19] Bovine chondrocytes were utilized with the nude mouse model since large numbers of cells can be readily obtained. The total amounts of GAG and collagen in the tissue engineered neocartilage were similar to cartilage synthesized in bioreactors on PGA scaffolds *in vitro* and cartilage formed *in vivo* using PEO alone.[7, 19] The fraction of type II collagen was reduced compared to native articular cartilage. While GAG contents decreased with increasing PEODM, total collagen increased, suggesting that the more mechanically stable networks with a higher crosslinking density (40% PEODM) may be utilized as scaffolds for neocartilage formation.

The tissue structure observed in the histology sections resemble neocartilage for all of polymer compositions studied and demonstrate a heterogeneous cell population (Figure 4.9). Cells are ovoid or elongated and trapped in lacunae similar to natural neocartilage. Control polymer implants showed no evidence of cartilage suggesting that cartilage formed from encapsulated chondrocytes and cell recruitment did not occur. Control

polymers demonstrated a typical foreign body response comprised of macrophages and giant cells in a fibrous capsule surrounding the implant. The presence of elongated cells (and the ratio of type I versus II collagen) is suggestive of partial dedifferentiation of the articular chondrocytes to fibrochondrocytes. Normal articular cartilage produces only type II collagen. Ectopic (subcutaneous) implantation of the constructs may be the cause of the cartilage dedifferentiation. Normal articular cartilage is exposed to mechanical forces and growth factors in the joint, which help to maintain the structure and function of the cartilage. The lack of presence of these stimuli, both mechanical and chemical, in the ectopic (subcutaneous) site of implantation may be responsible for the dedifferentiation of the tissue-engineered neocartilage. Mitotic (dividing) cells are observed in all sections (Figure 4.9). The PEODM network, most notably in the 30 and 40% PEODM polymer compositions, stained violet (Figure 4.9c,d). Chondrocytes trapped within the polymer present in the 40% PEODM constructs are viable. Necrosis is not observed.

4.5 Conclusion

Transdermal photopolymerization provides a minimally invasive method for injectable implantation of a hydrogel network. Chondrocytes survive encapsulation and subcutaneous implantation using photopolymerization and produce extracellular matrix forming neocartilage. The GAG and total collagen content of the neocartilage are similar to other tissue-engineered cartilage after 6 weeks of subcutaneous implantation. Future research is aimed at determining the maximal PEODM content where cell and tissue viability is maintained and studying the effects of long term implantation on the cartilage

implants. In addition, other cell types may be encapsulated to engineer other tissues in a similar fashion.

4.6 References

1. Langer R, Vacanti J. Tissue Engineering. *Science* 260: 920-926, 1993.

2. Freed L, Vunjak-Novakovic G. Tissue Engineering of Cartilage. In: Bronzind J, ed. *The Biomedical Engineering Handbook.* Boca Raton: CRC, pp. 1778-1796, 1995.

3. Nerem R. Cellular Engineering. *Ann Biomed Eng* 19: 529, 1991.

4. Vacanti CA, Langer R, Schloo B, Vacanti JP. Synthetic polymers seeded with chondrocytes provide a template for new cartilage formation. *Plastic and Reconstructive Surgery* 88 (5): 753-759, 1991.

5. Chesterman PJ, Smith AU. Homotransplantation of articular cartilage and isolated chondrocytes. *Journal of Bone Joint Surgery* 50B: 184, 1968.

6. Paige KT, Cima LG, Yaremchuk MJ, Vacanti JP, Vacanti CA. Injectable Cartilage. *Plastic and Reconstructive Surgery* 96 (6): 1390-1400, 1995.

7. Sims D, Butler P, Casanova R, Lee B, Randolph M, Lee WPA, Vacanti C, Yaremchuk M. Injectable cartilage using polyethylene oxide polymer substrates. *Plastic and Reconstructive Surgery* 98 (5): 843-850, 1996.

8. Kim WS, Vacanti JP, Cima L, Mooney D, Upton J, Puelacher WC, Vacanti C. Cartilage engineered in predetermined shapes employing cell transplantation on synthetic biodegradable polymers. *Plastic and Reconstructive Surgery* 94 (2): 234-239, 1994.

9. Elisseeff J, Sims D, Anseth K, Langer R. Transdermal Photopolymerizations. *in press,* PNAS .

10. Farndale R, Buttle D, Barrett A. Improved quantitation and discrimination of sulphated glycosaminoglycans by the use of dimethylmethylene blue. *Biochim Biophys Acta* 883 (173), 1986.

11. Woessner JF. The determination of hydroxyproline in tissue and protein samples containing small proportions of this imino acid. *Archiv. Biochem. & Biophys.* 93: 440-447, 1961.

12. Kim Y, Sah R, Doong J, al e. Fluorometric assay of DNA in cartilage explants using Hoechst 33258. *Anal Biochem* 174: 168, 1988.

13. O'Driscoll SW, Salter RB, Keeley FW. A Method for quantitative analysis of ratios of types I and II collagen in small samples of articular cartilage. *Analytical Biochemistry* 145: 277-285, 1985.

14. Decker C. UV-Curing Chemistry: Past, Present and Future. *Journal of Coatings Technology* 59 (751): 97-106, 1987.

15. Hill-West J, Chowdhury S, Sawhney A, Pathak C, Dunn R, Hubbell J. Prevention of postoperative adhesions in the rat by in situ photopolymerization of bioresorbable hydrogel barriers. *Obstet Gynecol* 83 (1): 59-64, 1994.

16. Hill-West J, Chowdhury S, Slepian M, Hubbell J. Inhibition of thrombosis and intimal thickening by in situ photopolymerization of thin hydrogel barriers. *Proc Natl Acad Sci USA* 91 (13): 5967-71, 1994.

17. Langer R, Elisseeff J, Anseth K, Sims D. Semi-Interpenetrating or Interpenetrating polymer networks for drug delivery and tissue engineering. US Patent #08/862,740, May 1997.

18. Brannon-Peppas L. *Preparation and characterization of crosslinked hydrophilic networks*. Washington, DC: ACS, 1994.

19. Freed L, Vunjak-Novakovic G, Biron R, Eagles D, Lesnoy D, Barlow S, Langer R. Biodegradable polymer scaffolds for tissue engineering. *Bio/technology* 12, 1994.

Chapter 5. Controlled-Release of Growth Factors in Photopolymerized Hydrogels*.

5.1 Introduction

The previous two chapters examined the ability to tissue engineer cartilage in a photopolymerizing hydrogel both *in vitro* and *in vivo*. While cartilage-like tissue formed, the collagen contents, particularly in *in vitro* samples, were far below those of native cartilage. Growth factors help form and maintain normal articular cartilage and may prove useful in stimulating matrix production. This chapter examines 1.) the ability to encapsulate growth factors in PLGA microspheres and 2.) the effects of encapsulated growth factors on cartilage formation in photopolymerized hydrogels.

5.2 Background

Insulin-like growth factor (IGF) exerts anabolic effects on cells of mesenchymal origin, particularly fibroblasts and chondrocytes.[1] IGF causes cell proliferation and extracellular matrix (ECM) synthesis, both crucial processes for cartilage tissue engineering. IGF is synthesized locally within chondrocytes and is stored in the ECM. IGF interacts with other growth factors, including synergistic interactions with epidermal growth factor (EGF). Of particular interest to cartilage homeostasis *in vivo* and cartilage tissue engineering is the synergistic effects between IGF and transforming growth factor-beta (TGF-b).[2]

TGF-b has many biological actions. *In vitro* effects of TGF-b have been difficult to ascertain due to often-contradictory results.[1] In cartilage TGF-b inhibits cell

* This chapter will be submitted in part for publication in a peer-reviewed journal.

proliferation and stimulates ECM production.[1] The inhibition in cell proliferation was overcome when IGF and TGF were combined *in vitro.* Tsukazaki et al found a synergistic effect of IGF-1 and TGF-b, causing a 10-fold increase in DNA synthesis on plated chondrocytes when present in a 25:1 (ng/ml) ratio.[3] This synergy was studied in an experimental group in this chapter.

The ability to mimic the native local environment of a chondrocyte may be aided by the addition of growth factors to a tissue engineering scaffold system. Growth factors can be added to a system using a variety of methods.[4] A growth factor may be incorporated into a tissue engineering scaffold via encapsulation in polymer fibers or matrix. The growth factor may also be covalently attached to the scaffold using a variety of chemistries. The kinetics of growth factor release in a system is another critical factor in obtaining the desired effect of a growth factor. Cellular responses may differ when a bolus versus controlled release growth factor is presented.[5]

Polymeric microspheres can release proteins over an extended period of time (controlled release).[6] Poly(D,L-lactic-*co*-glycolic acid) (PLGA) microspheres have been used extensively for controlled release with tissue compatibility and biodegradability.[7] Microspheres are injectable and release in a localized site. These two properties are important for their use in the photopolymerizing hydrogel system. First, the hydrogel system was developed to provide a minimally invasive cartilage tissue engineering system that can be implanted through an injection. Microspheres could be injected and photopolymerized with the polymer hydrogel system. Second, local delivery of growth

factors is crucial since these proteins often have short half-lives and multiple biological effects with potential systemic toxicity. [4] The purpose of this work was to 1.) release growth factors in a controlled release manner in the photopolymerizing hydrogel and 2.) examine the effects of the growth factors on encapsulated chondrocytes.

5.3 Methods

5.3.1. Microsphere Preparation. Microspheres were prepared by a double emulsion technique.[8] Two hundred mg poly(lactic acid-*co*-glycolic acid), PLGA 50:50 was dissolved in 1 ml of methylene chloride. IGF-1 (50, 100 and 200 μl of 10μg IGF-1/ml stock, R&D Systems, **612**) and TGF-b (100 of 1μg TGF-b/ml stock, R&D Systems) were added to the PLGA solution. These microsphere groups will subsequently be referred to as IGF50, IGF100, IGF200 and TGF100 respectively. One group included a combination of IGF100 and TGF100 microspheres (IGF/TGF) in a 25:1 ratio at a concentration of 15 mg/ml of microspheres. The IGF-1 stock solution was 10 mM acetic acid with 0.1% bovine serum albumin. The TGF-b stock solution was 4 mM HCl and 1 mg/ml bovine serum albumin. The polymer and growth factor were sonicated on ice for 6 pulses, 50% duty output 3 microtip (Vibracell, Danbury, CT). This primary emulsion was then added to a 100-mL aqueous solution of 1% (w/v) poly(vinyl alcohol) (PVA). The second emulsion was formed by homogenization for 1 min at 3,000 rpm on a Silverson (East Longmeadow, MA) homogenizer using a 5/8" micro-mixing assembly with a general with a general-purpose disintegrating head. The resultant water-in-oil-in-water (w/o)/w emulsion was stirred continuously for 3 h for solvent evaporation. The hardened

spheres were centrifuged, washed 3 times with distilled water and freeze dried for 48 hours and stored under desiccant at –20°C.

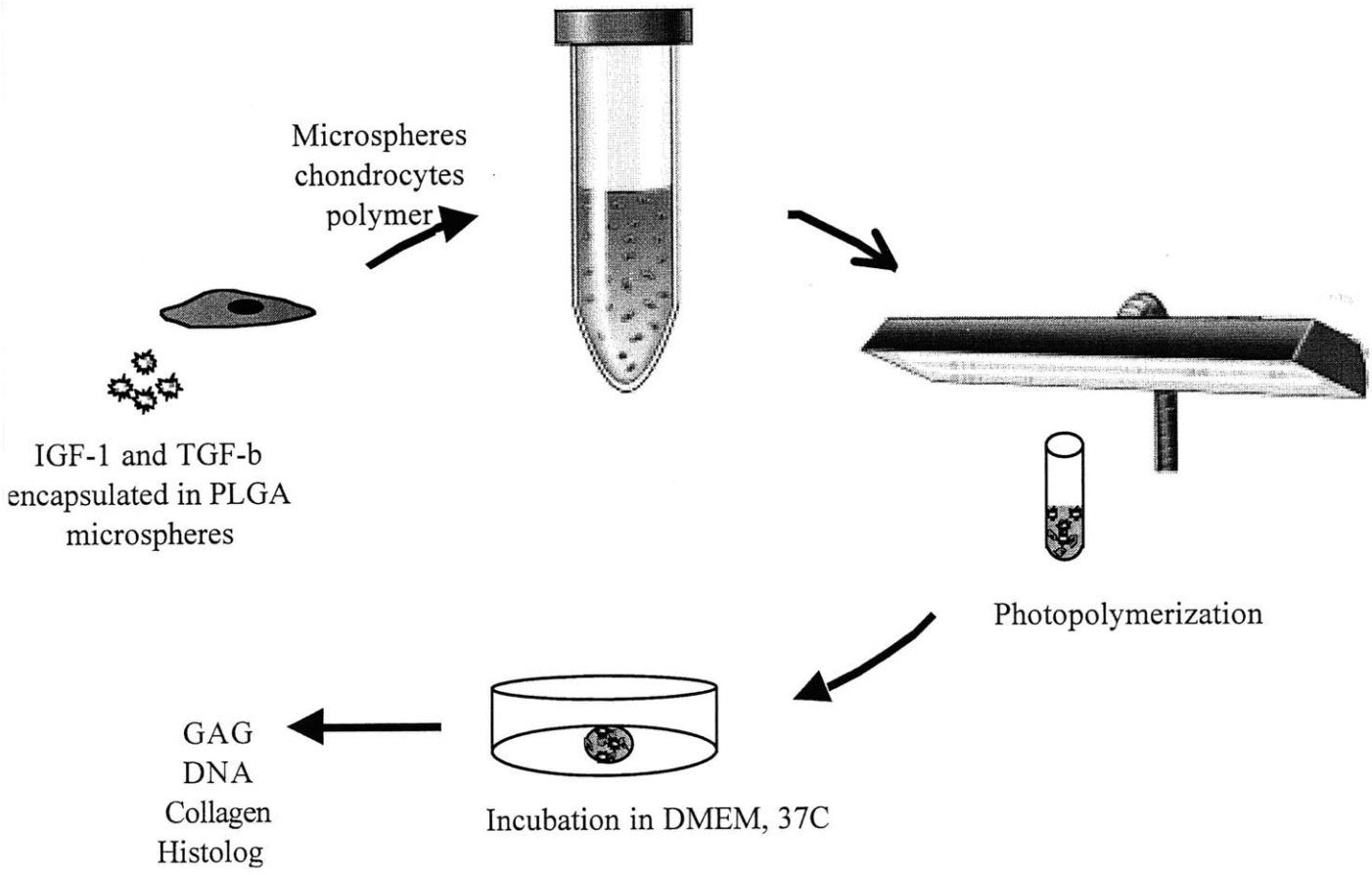

Figure 5.1. Schematic of microsphere encapsulation and experiment.

Microsphere loading was determined by protein assay. Approximately 10 mg of microspheres were degraded in 2 ml of 0.1N NaOH and 0.5% SDS on an orbital shaker at 37°C overnight. Protein content was subsequently determined by a micro BCA protein assay (Pierce, Rockford, IL).

Release. Approximately 10 mg of microspheres were placed in Eppendorf vials with 1 ml PBS. The spheres were incubated statically at 37°C. The PBS was removed, frozen and replenished at 1, 2, 5, 10 and 15 days. ELISAs (enzyme linked immunosorbant assay) for IGF-1 (Oxford Diagnostics) and TGF-b (R&D Systems) were performed on the spent PBS to determine the concentration of active protein released. Blank microspheres (containing PBS in place of growth factor stock) were synthesized and released as controls.

5.3.2. Chondrocyte Encpasulation. PEODM (MW 3400, Shearwater Polymers) and PEO (MW 100,000, Shearwater Polymers) were dissolved in PBS in a 2:3 ratio (40% PEODM) to make a final polymer concentration of 20% (w/v) in phosphate buffered saline (PBS). Photoinitiator (hydroxycyclohexyl phenyl ketone, HPK, Polysciences, Warrington, PA) was added to make a final concentration of 0.03% (w/v). Primary bovine chondrocytes were harvested and isolated from the calf femoropatellar groove as described. (Chapter 3) The polymer solution was added to a cell pellet to make a final concentration of $50x10^6$ cells/cc.

IGF, TGF and FGF were dissolved in the PEODM polymer and cell suspension at concentrations of 50, 30 and 3 ng/ml, respectively. The cells and growth factor and polymer were photopolymerized as described previously in Chapter 3. Constructs were

incubated under static conditions at 37°C. Specimens were removed for biochemical analysis at 3, 9 and 18 days.

Fifteen milligrams of microspheres were suspended and mixed in 1 ml of polymer/cell solution. Control groups included polymer without cells or microspheres, polymer with chondrocytes and no microspheres, and polymer with cells and blank spheres. Experimental growth factor groups included IGF100, IGF200, TGF200 and IGF/TGF spheres combined in a 25:1 ratio. The polymer/cell suspension was mixed on a rotating plate for one hour. The suspension was subsequently aliquoted (150 μl) in sterile Eppendorfs. The solutions were photopolymerized by placement under a UVA lamp (Glomark Systems, Upper Saddle River, NJ). The lamp was at a height such that the solutions received 1.5 mW/cm^2 for 3 minutes as measured by a radiometer. All constructs were incubated in 12-well tissue culture plates with complete media (high glucose DMEM, 10% FBS, 10 μg/ml vitamin C, 12.5 mM HEPES, 0.1 mM nonessential amino acids and 0.4 mM proline) at 37C/5% CO_2 under static conditions.

Constructs were removed at 3, 7, 10 and 14 days for the IGF spheres (n=4-6) and at 14 days only for the TGF and TGF/IGF spheres (n=4). Constructs were removed from the tissue culture plates, blotted dry and wet weights (ww) were obtained. Gels were subsequently lyophilized for at least 48 hours after which dry weights (dw) were determined. The hydrogels were digested in 1 ml papainase overnight at 60°C . GAG content was estimated by chondroitin sulfate using dimethylene blue dye and a UV-VIS spectrophotometer.[9] Total collagen content was determined by the hydroxyproline

determined after acid hydrolysis and reaction with p-dimethylaminobenzaldehyde and chloramine-T using 0.1 as the ratio of hydroxyproline to collagen.[10] The cell content of the hydrogels was determined using Hoechst 33258, spectrofluorometry and a conversion factor of 7.7 pg DNA per chondrocyte.[11] At specified time points, constructs were removed from the wells. The constructs were blotted dry and weighed to obtain wet weights. After two days of vacuum drying construct dry weights were obtained. The dried constructs were digested with papain and frozen for analysis. GAG, DNA and collagen contents were determined using DMMB dye, fluroscopy and hydroxyproline contents, respectively, as described.[9, 11] Histology was prepared according to standard histological technique.

One and two-way ANOVA analysis of variance was performed using Minitab Software.

5.4 Results

5.4.1. Release. The cumulative release of IGF was dependent on the initial microsphere loading. The release curves for both IGF1 and TGFb exhibited no initial bursts. The IGF1 spheres loaded with lower concentrations of growth factor demonstrated a release plateau after one week whereas the IGF200 and TGFb spheres showed continued release over the two-week time period studied. The IGF200 microspheres released 125 ng/ml of active IGF over 15 days, more than double the IGF100 spheres that released 55 ng/ml over the same time period (Figure 5.2). The TGF spheres released 200 pg/ml of active

protein over 15 days (Figure 5.3). The total protein loading of the IGF and TGF microspheres was 14.95±0.72 and 0.48±0.13 ng/mg respectively.

5.4.2. Chondrocyte Encapsulation. Gels made with 15 mg/ml of microspheres were similar in form to control gels without microspheres except for increased opacity from the microspheres. Microspheres encapsulated at a concentration of 30 mg/ml interfered with hydrogel formation, producing gels that were not as mechanically stable as control gels and those synthesized with 15 mg/ml.

GAG and total collagen contents increased over the two-week incubation period. GAG contents among the experimental groups were similar over the first three time points up to 10 days. A statistically significant increase in GAG between control constructs and those with 15 mg/ml IGF100 microspheres was present after 14 days ($p=0.013$, Figure 5.4). The total collagen contents did not differ

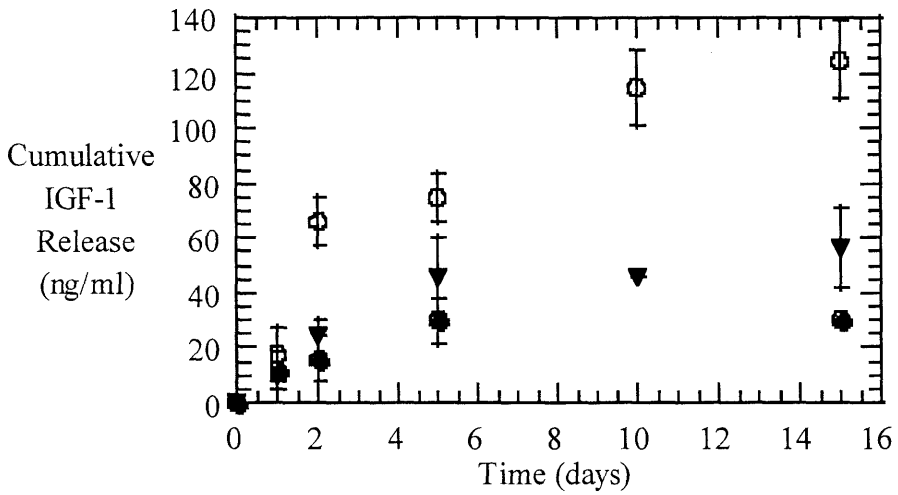

Figure 5.2. Cumulative release of IGF-1 from PLGA microspheres prepared with 50 (--●--), 100 (--▼--) and 200 ul (–○--) of stock.

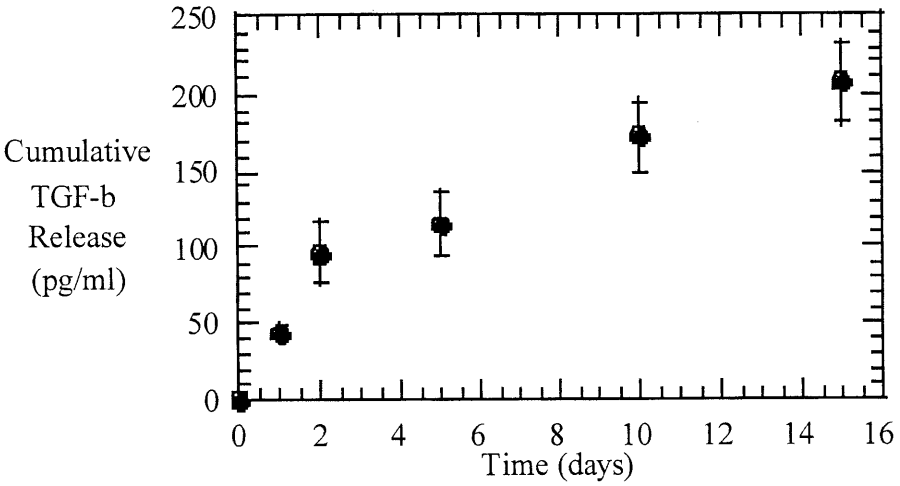

Figure 5.3. Cumulative release of TGF-b from PLGA microspheres.

between the polymer, blank, 15 and 30 mg/ml groups over the two weeks studied ($p=0.22$, Figure 5.5). There was a significant decrease in DNA content from 3 to 7 days in all of the experimental groups ($p=0.04$). The DNA content appeared to stabilize after one week with no significant decreases among any group found from 7 to 14 days ($p=0.40$, Figure 5.6).

Further experimental groups studied showed a significant increase in GAG production at 14 days in the (IGF/TGF, $p=0.04$, Figure 5.7). A decreased total collagen content was observed in the IGF/TGF group (Figure 5.8). The IGF/TGF group showed a significantly increased DNA content (Table 5.1). All other experimental groups had similar total collagen and cell contents.

Figure 5.9(a-e) demonstrates histological sections of the tissues formed after 14 days of incubation. Figure 5.9a shows the encapsulated chondrocytes with no microspheres present. Ovoid and elongated cells are distributed within an extracellular matrix. The extracellular matrix is lightly basophilic. As described in Chapter 3, the cells show multiple cell distributions with areas of dense cellularity characteristic of cartilage and areas of low cell dispersion. Figures 5.9b and c show cells encapsulated with IGF microspheres. No gross difference with the polymer alone (Figure 5.9a) or blank microspheres (section not shown) is apparent. The microspheres can be easily seen on higher magnification (Figure 5.9c). A large difference in matrix staining is observed in the IGF/TGF encapsulated cells (Figures 5.9d-e). The pericellular regions show an increased basophilic staining. Furthermore, there appears to be a more even (and dense) cell

distribution compared to the other sections. Entrapped bubbles are observed as round, clear regions (Figures 5.9d and 3).

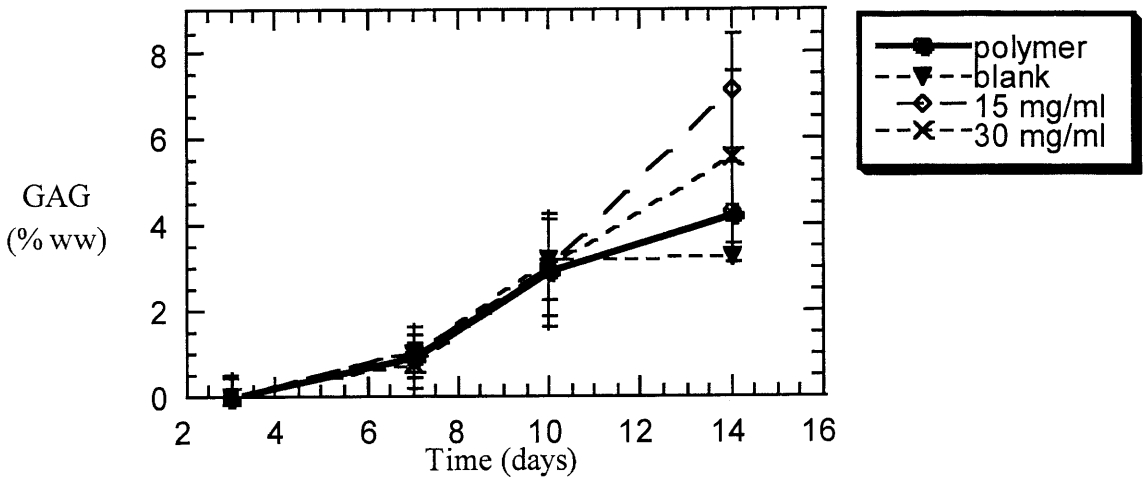

Figure 5.4. Evolution of %GAG with time for hydrogel control, blank spheres, 15 and 30 mg/ml IGF100 spheres.

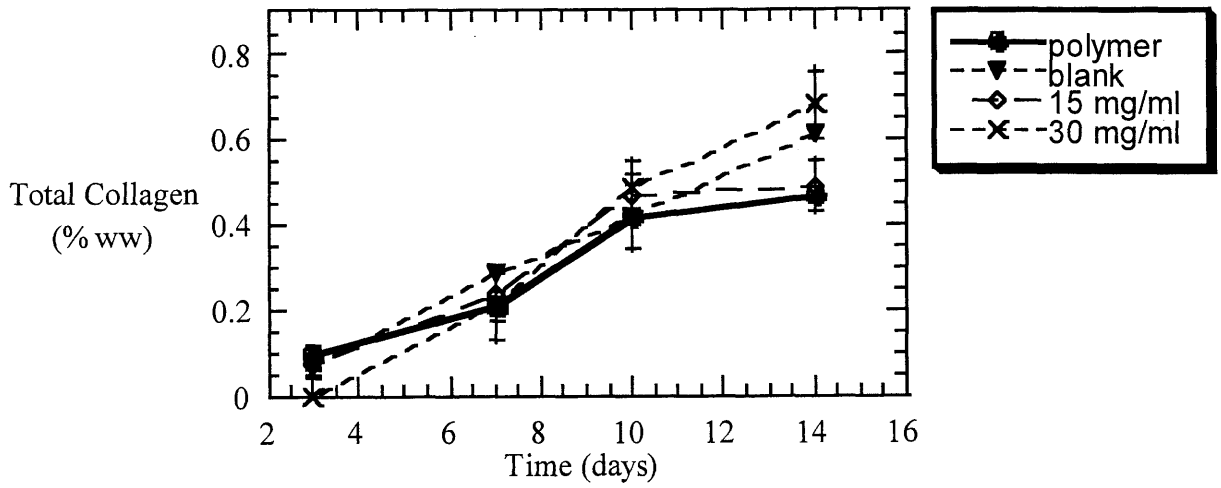

Figure 5.5. Evolution of %total collagen with time for hydrogel control, blank spheres, 15 and 30 mg/ml IGF100 spheres.

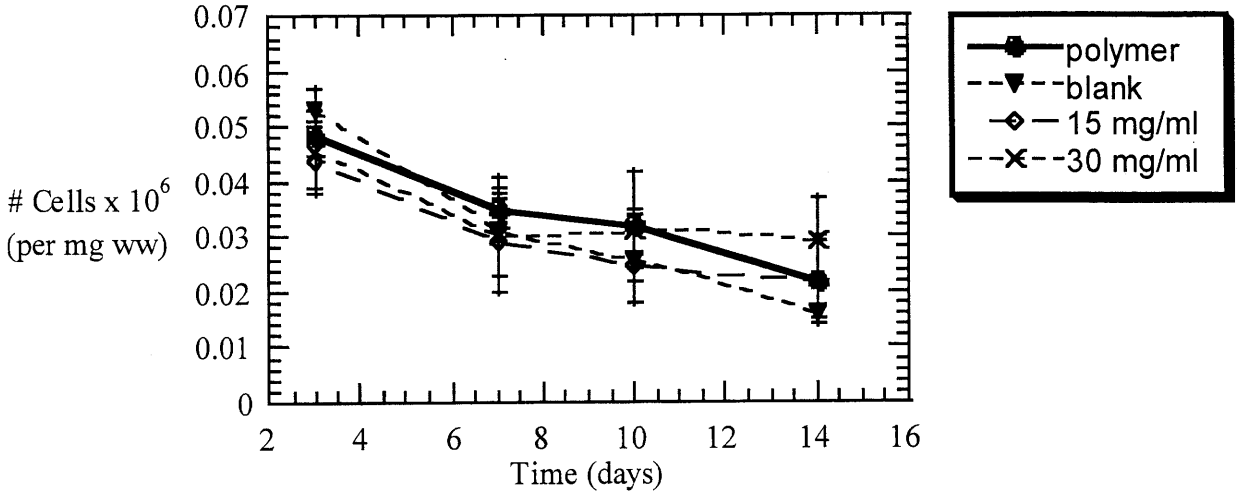

Figure 5.6. Cell content of constructs for hydrogel control, blank spheres, 15 and 30 mg/ml IGF100 spheres.

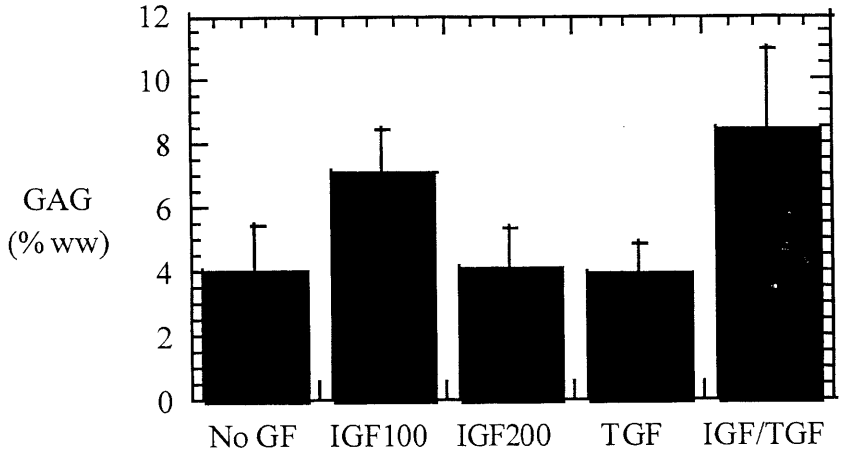

Figure 5.7. Comparison of % GAG among growth factor groups at 14 days.

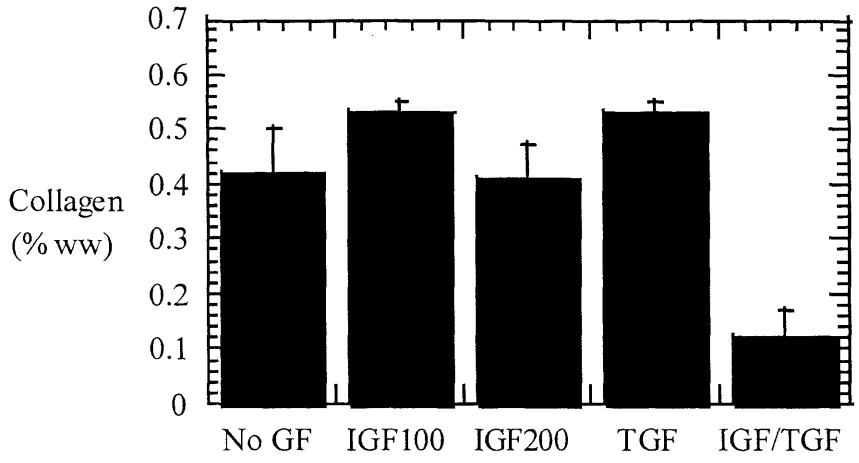

Figure 5.8. Comparison of % total collagen among growth factor groups at 14 days.

A.

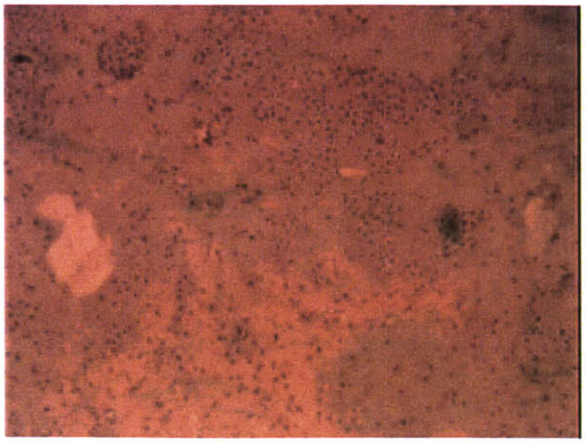

B.)

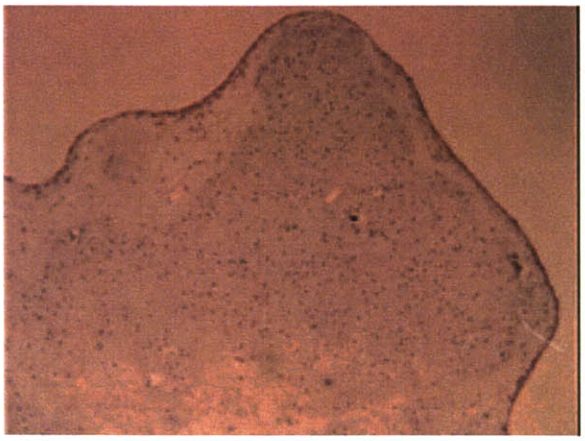

C.)

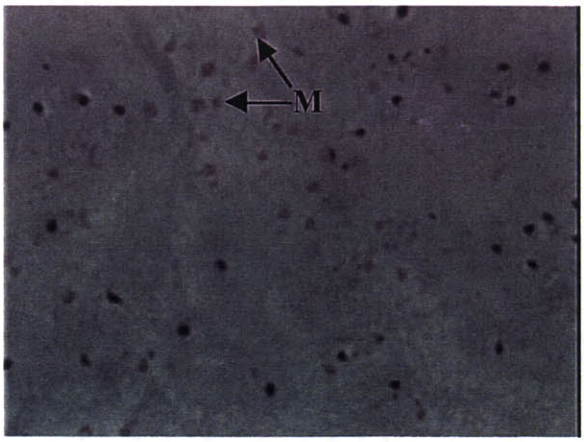

D.

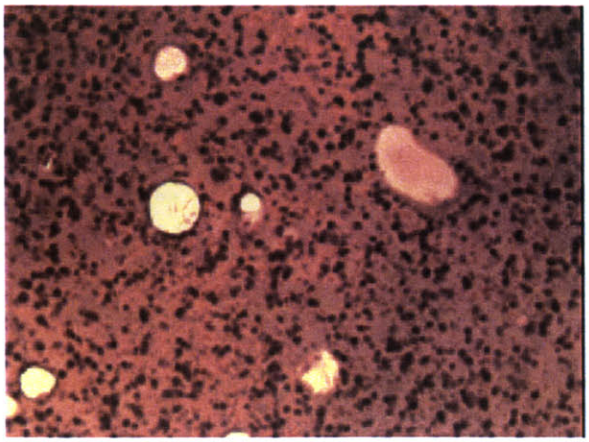

E.)

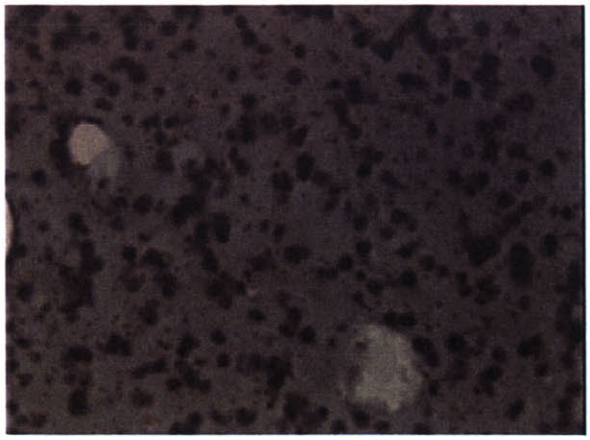

Figure 5.9. H&E sections of day 14 tissue polymerized with a.) no microspheres (100X), b.) IGF100 microspheres 100X, and c.) 400X, d.) IGF/TGF microspheres (100X) and e.) 200X.

5.5 Discussion

Chondrocytes experience biochemical and mechanical stimulation *in vivo* that are integral to the development and maintenance of cartilage.[12] Mechanical forces stimulate chondrocytes to produce and maintain their extracellular matrix.[13] Long-term disuse of a joint can lead to atrophy. Growth factors aid in signaling and regulating cartilage development and extracellular matrix maintenance.[14] Growth factors are stored in the matrix for immediate release when needed. Similarly, the purpose of this work was to store growth factors in a synthetic matrix in the form of microspheres to aid in cartilage development in photopolymerized hydrogels.

Polymeric microspheres serve a critical role in a variety of biomedical applications, providing localized, controlled delivery of sensitive molecules such as growth factors.[7] TGF-beta and basic fibroblast growth factor (bFGF) have been encapsulated in polymeric microspheres to study cellular response in vascular tissue engineering.[5] To our knowledge, IGF-1 has not been encapsulated in a microsphere system. IGF-1 has a multitude of clinical applications that may be better served with a controlled release delivery system.[15, 16]

The PEO-based hydrogels that were utilized for photoencapsulation must have porous structure large enough to allow nutrient and waste transport for cell metabolism. See swelling (Chapter 4) and mechanical (Chapter 3) data. Small proteins, such as growth factors, can easily diffuse in the hydrogel matrix. IGF1 and TGFb encapsulated directly in the hydrogel provided no benefit to GAG and DNA concentrations over 18 days (data

not shown). For this reason microspheres were embedded in the hydrogel to provide controlled release of relevant growth factors for encapsulated chondrocytes. The concentration of growth factor may be easily changed by the amount of microspheres encapsulated.

Differences in GAG production appear after two weeks of *in vitro* incubation. Differences of over 2% (ww) GAG are observed with IGF100 and IGF1/TGFb microsphere groups compared to controls. On the other hand, collagen levels remain low. While differences in mean collagen between experimental groups appear to be increasing with the largest difference apparent at 14 days, no statistical difference was observed. Longer incubations may find a positive effect of IGF1 or TGFb on collagen production.

DNA contents decreased over the experimental time period. This decrease in DNA content was discussed in Chapter 3. The most significant growth factor effect was on the DNA content in hydrogels with IGF1 and TGFb microspheres. The microspheres were combined in a ratio (25:1) found to increase DNA synthesis 10-fold.[3] The photoencapsulated cells showed a similar 10-fold increase in cell content. While the GAG content in these hydrogels was significantly above control gels, the collagen content was significantly lower. The chondrocytes encapsulated with IGF1/TGFb spheres were stimulated to multiply but at the expense of matrix synthesis. The histological sections of the IGF1/TGFb constructs provide information on the potential matrix production.

Histologically the IGF1/TGFb constructs show marked differences from controls and IGF1 constructs. The increased cell content can be visually confirmed in the IGF1/TGFb sections. More importantly, the pericellular region of the chondrocytes

stained strongly for proteoglycan synthesis. This increased pericellular staining suggests that the chodrocytes are actively producing matrix. Thus, it may be hypothesized that longer incubation may demonstrate a significant increase in GAG and collagen production in the IGF1/TGFb constructs.

Rigorous mixing is important for proper cell distribution within the viscous prepolymer solution. The addition of microspheres to the prepolymer further increases the necessity for proper mixing before polymerization. Mixing (via pipette, vortex or manual stirring) causes air bubbles in the viscous prepolymer solution. Due to the high viscosity of the prepolymer solution, these air bubbles may still be present during photopolymerization. The histology sections (Figure 5.9) demonstrate air bubbles trapped during polymerization. These bubbles demonstrate interesting properties of the hydrogel. First, the shape of the small bubbles is maintained by the hydrogel after polymerization. Second, the tissue maintains the shape of the hydrogel scaffold and does not grow into the bubble space. This suggests that the hydrogel may be used to tissue engineer complex shapes. For example, air bubbles of different sizes may be forced into the prepolymer using airflow at different rates and photopolymerized. This would create a hydrogel with a large porous structure in addition to the microscopic pores formed by the polymer chains. Cells may be encapsulated during the photopolymerization and/or cells could be seeded on the large pores.

Further study should focus on optimizing the growth factor release characteristics for chondrocyte division when cells are initially encapsulated and subsequent matrix synthesis. For example, an initial or periodic burst of a combination of growth factors

may stimulate increased matrix production. Increased collagen production would be highly beneficial to the constructs since their collagen content was far below native values.

5.6 References

1. Humbel, R.E. in *Hormonal Proteins and Peptides* (ed. Li, J.) (Academic Press, NY, 1984).

2. Malemud, C.J., The Role of Growth Factors in Cartilage Metabolism. *Osteoarthritis* **19**, 569-581 (1993).

3. Tsukazaki, T., *et al.*, Effect of Transforming Growth Factor-beta on the Insulin-Like Growth Factor-I Autocrine/Paracrine Axis in Cultured Rat Articular Chondrocytes. *Experimental Cell Research* **215**, 9-16 (1994).

4. Baldwin, S. & Saltzman, W., Materials for protein delivery in Tissue Engineering. *Advanced Drug Delivery Reviews* **33**, 71-86 (1998).

5. Dinbergs, I., Brown, L. & Edelman, E., Cellular Response to Transforming Growth Factor-b1 and Basic Fibroblast Growth Factor Depends on Release Kinetics and Extracellular Matrix Interactions. *Journal of Biological Chemistry* **271**, 29822-29 (1996).

6. Langer, R. & Moses, M., Biocompatible Controlled Release Polymers for Delivery of Polypeptides and Growth-Factors. *Journal of Cellular Biochemistry* **45**, 340-345 (1991).

7. Langer, R., New Methods in Drug Delivery. *Science* **249**, 1527-1533 (1990).

8. Cohen, S., Yoshioka, R. & Langer, R., Controlled delivery systems for proteins based on poly(lacitc/glycolic acid) microspheres. *Pharm Res* **8**, 713-720 (1991).

9. Farndale, R., Buttle, D. & Barrett, A., Improved quantitation and discrimination of sulphated glycosaminoglycans by the use of dimethylmethylene blue. *Biochim Biophys Acta* **883**, 173-177 (1986).

10. Woessner, J.F., The determination of hydroxyproline in tissue and protein samples containing small proportions of this imino acid. *Archiv. Biochem. & Biophys.* **93**, 440-447 (1961).

11. Kim, Y., Sah, R., Doong, J. & al, e., Fluorometric assay of DNA in cartilage explants using Hoechst 33258. *Anal Biochem* **174**, 168 (1988).

12. Buckwalter, J. & Mankin, H., Articular Cartilage. Part I: Tissue Design and Chondrocyte-Matrix Interactions. *Journal of Bone and Joint Surgery* **79-A**, 600-611 (1997).

13. Grodzinsky, A. & Urban, J. in *Interstitium, Connective Tissue and Lymphatics* 67-84 (Portland Press, Ltd., London, 1995).

14. Hill, D. & Logan, A., Peptide growth factors and their interactions during chondrogenesis. *Progress in Growth Factor Research* **4**, 45-68 (1992).

15. Trippel, S., Growth Factor Actions on Articular Cartilage. *Journal of Rheumatology* **22**, 129-131 (1995).

16. Baxter, R., The somatomedins: insulin-like growth factors. *Adv. Clin. Chem.* **25**, 49-115 (1987).

Chapter 6. Conclusions, Implications and Future Work

The aims of this thesis were to 1.) develop, describe and test a novel, minimally invasive method for implanting hydrogels which has been termed transdermal photopolymerization and 2.) apply transdermal photopolymerization to engineering cartilage tissue. The results described in this dissertation demonstrate the feasibility and efficacy of transdermal photopolymerization. Various biomedical applications of transdermal photopolymerization, including tissue engineering, were examined.

Conclusions

Transdermal Photopolymerization. The studies in this thesis have demonstrated the feasibility of transdermal photopolymerization. Photopolymerization can proceed under tissues with thickness comparable to those found in humans. Polymerization times determined by kinetic analysis are clinically feasible, with only minutes of light exposure required to polymerize. Toxicity studies yielded the conditions required to successfully encapsulate cells with undetected or minimal damage. Further *in vivo* work demonstrated the feasibility and biocompatibility of transdermal photopolymerization in mice and rats.

Cartilage Tissue Engineering. Initial photoencapsulation experiments demonstrated cell survival during the photoencapsulation. Further analysis of the hydrogels incubated *in vitro* demonstrated extracellular matrix deposition that increased over time. In addition, the matrix increased in mechanical function.

Growth factors relevant to cartilage development and maintenance were released from synthetic microspheres embedded in the hydrogel. The presence of the growth

factors in the hydrogel increased DNA and GAG contents but did not significantly alter collagen contents.

The potential of cartilage tissue engineering using transdermal photopolymerization was further demonstrated by the production of cartilage-like tissue *in vivo*. SemiIPNs implanted subcutaneous in athymic mice increased extracellular matrix (GAG and collagen) over the 7 week time period studied.

Implications and Future Work

As described in Chapter 2, the development of transdermal of transdermal photopolymerization has a wide range of applications. Drug delivery and tissue engineering applications were examined in this thesis, with a focus on cartilage tissue engineering. The hydrogel matrix may be ideal for engineering other tissue types. Pilot experiments have also been performed using the photopolymerizing hydrogel as a "living" cartilage glue. Tissue engineered, autologous or allogenic cartilage that is placed in a cartilage defect must integrate with the host cartilage to become fully functional. The hydrogel may act as a glue to prevent implant movement. Cells present in the hydrogel would help form tissue in the gap region between the two pieces of cartilage, promoting integration.

A wide range of photoreactive polymers and photoinitiators may be applied to the technique of transdermal photopolymerization. This opens further questions to the choice of scaffold (polymer) and the biology of the chondrocyte interaction with the gel. The interactions of cells entrapped within a gel may be different than those seeded on a gel or solid scaffold. The morphology, gene expression, and general biology of cells entrapped

within a gel should be examined. In particular, varying the chemistry of the gel entrapping the chondrocytes and analyzing the subsequent cell biology may provide useful insight for cartilage development and engineering. Potential chemistry alterations to the gel system are numerous.

As described in Chapter 2, visible light penetrates tissue more easily than UVA light. Defining efficient visible light photoinitiating systems may allow use of visible light for transdermal photopolymerization. Analysis of biocompatibility and kinetics of new visible light initiating systems is necessary for the efficient use of transdermal photopolymerization for hydrogel implantation.

In order for the clinical application of transdermal photopolymerization and photoencapsulation, further toxicity issues should be examined. While this thesis examined potential radical damage to cell membranes, further work should probe other possible mutations. Potential protein oxidation and DNA damage in encapsulated cells and cells adjacent to the implant should be studied. For example, the presence of mutated bases or unscheduled DNA synthesis may be analyzed.

Appendix A. Kinetic program used for photopolymerization modeling.

```
C  KINETIC PROGRAM WITH DARK POLYMERIZATION BUT NO PULSE
C  Makes thin film approximation for initiation
c
c  Kinetic modelling of the polymerization reaction
involving systems
c     exhibiting a gel effect and prediction of the
c     kinetic constants of the system as a function of the
free volume of
c     the system.
c
c
c Variable description:
c
c  Kinetic constants:
c
c   Ksubp       - kinetic constant for propagation, function
of free volu
c   Ksubp0      - parameter for determining ksubp
c   vsubf0      - critical free volume for ksubp
c   Vstar       - parameter for determination of ksubp
c   Ksubt       - kinetic constant for termination, function
of free volu
c   Ksubt0      - parameter for determining ksubt
c   vsubfc      - critical free volume for ksubt
c   A           - parameter for determination of ksubt
c   ratio       - parameter that relates the reaction
diffusion resistance
c                 to the propagation reaction
c
c  Volume contraction and free volume:
c
c   vsubf       - actual free volume of the system, function
of time
c   vsubfeq     - equilibrium free volume, function of
conversion
c   v           - specific volume
c   vm          - monomer specific volume
c   vp          - polymer specific volume
c   epsilon     - fractional change in volume from monomer
to polymer
c   veq         - equilibrium specific volume, assumed
linear with conver
c   phip        - polymer volume fraction
c   alpham      - thermal expansion coefficient of the
monomer
```

```
c   alphap      - thermal expansion coefficient pf the
polymer
c   glasstm     - glass transition temperature of the
monomer (celcius)
c   glasstp     - glass transition temperature of the
polymer (celcius)
c
c  Reaction concentrations and conditions:
c
c   concI       - initiator concentration
c   concI0      - initial initiator concentration
c   concM       - monomer concentration
c   concM0      - initial monomer concentration
c   concMr      - concentration of growing polymer radicals
c   concrr      - concentration of initiator radicals
c   time        - reaction time in seconds
c   timetot     - total time of reaction observation
c   timeinc     - length of time in each finite difference
c   ntime       - total number of time increments
c   temp        - reaction temperature
c   X           - conversion
c   f           - initiator efficiency
c
c  Dummy variables:
c
c   R
c   S
c
c
c
c Begin Program
c
c   Declarations
c
      DOUBLE PRECISION
KSUBP,KSUBT,KSUBI,V,VEQ,VSUBF,VSUBFE,TAU,CONCI
      DOUBLE PRECISION
CONCM,X,PHIP,TIMEIC,CONCMR,TIME,RATEV
      DOUBLE PRECISION
AA,V1,EPSI,TIMIC2,TIMED,VX,V2,TAU1,TAU2
      DOUBLE PRECISION KEFF
      REAL ti,rv,rt,conv,freev,kt,kp
      REAL KSUBP0,VSUBF0,VSTAR,KSUBT0,VSUBFC,A,I0
      REAL ATAU,BTAU,ALPHAM,ALPHAP,GLASTM,GLASTP
      REAL CONCO2,TEMP,VM,VP,CONCI0,CONCM0
      REAL XCSUBP,XCSUBT,EPSILO,CONO20,F,RATIO
     INTEGER I,TIMETO,MM,K,L,M,nnn
```

```
c
c
c     Input Section
c
c
        READ *, KSUBP0,VSUBF0,VSTAR
        WRITE (*,*) KSUBP0,VSUBF0,VSTAR
        READ *, KSUBT0,VSUBFC,A,RATIO
        WRITE (*,*) KSUBT0,VSUBFC,A,RATIO
        READ *, I0,EPSI
        WRITE (*,*) I0,EPSI
        READ *, VM,VP
        WRITE (*,*) VM,VP
        READ *,ALPHAM,ALPHAP
        READ *,GLASTM,GLASTP,TEMP
        READ *,CONCI0,CONCM0
        READ *,TIMETO,TIMEIC
        READ *,F
        READ *, TIMED
        WRITE (*,*) ALPHAM,ALPHAP
        WRITE (*,*) GLASTM,GLASTP,TEMP
        WRITE (*,*) CONCI0,CONCM0,CONO20
        WRITE (*,*) TIMETO,TIMEIC
        WRITE (*,*) F
        WRITE (*,*) TIMED
        WRITE (*,*)
        WRITE (*,*) RATIO, VSUBF0
C
C
C      INITIALIZATION
C
C
        XINC = 0.01
        V = VM
        V1 = AFRAC*VM
        V2 = (1.-AFRAC)*VM
        X = 0.
        CONCM = CONCM0
        CONCI = CONCI0
        CONCMR = 0.
        CONCO2 = CONO20
        KSUBP = KSUBP0
        KSUBT = KSUBT0
        TIME = 0.
        RATE = 0.
        MM = 0
        VEQ = VM
```

```
        VSUBFE = 0.025 + ALPHAM*(TEMP-GLASTM)
        VSUBF = VSUBFE
        NPRINT = 5000
        WRITE (*,100) TIME,X,CONCMR,RATE,QSSH,V,VEQ
     .           ,VSUBF,VSUBFE
C
C
C     CALCULATIONS
C
C
        EPSILO = (VM-VP)/VM
        TIMIC2 = TIMEIC*250.
C
C
c   BEGIN CALCULATION LOOP
C
C
    3    CONTINUE
            TIME = TIME + TIMEIC
C
C       DETERMINATION OF V AND  VSUBF
C
            NT = NT + 1
            X = 1. - CONCM/CONCM0
            VEQ = VM*(1. - EPSILO*X)
            PHIP = X*(1.-EPSILO)/(1.-EPSILO*X)
            VSUBFE = 0.025 + ALPHAM*(TEMP-GLASTM)*(1.-PHIP)
      A     +ALPHAP*(TEMP-GLASTP)*PHIP
            VSUBF = VSUBFE

C
C        DETERMINATION OF KINETIC CONSTANTS
C
            KSUBP = KSUBP0 * (1.0+1.0/EXP(-VSTAR*
      c               (1./VSUBF-1./VSUBF0)))**-1.0
            KSUBT = KSUBT0 * ((((RATIO*KSUBP*CONCM/KSUBT0
      C             + EXP(-A*(1./VSUBF-1./VSUBFC)))**-1.0)
      C             + 1.0)**-1.0)
            KEFF = KSUBP/(KSUBT**0.5)
            VX = V
C
C        DETERMINATION OF CONCENTRATIONS --
C
            AA = I0*3.0512E-06*EPSI*CONCI*TIMEIC
            CONCI = CONCI-AA
            CONCMR = CONCMR*(1.-
KSUBT*CONCMR*TIMEIC*2.)+2.*AA*F
```

```
            QSSH = (-
CONCMR*KSUBT*CONCMR*TIMEIC*2.+2.*AA*F)/AA/2./F
            CONCM = CONCM -(KSUBP*CONCM*CONCMR)*TIMEIC
            XX = KSUBP*CONCM*CONCMR*TIMEIC
            IF (XX.GT.XMAX) THEN
               XMAX = XX
            ELSEIF (XX.LT.XMAX/100.) THEN
               TIMEIC = TIMIC2
               XINC = 0.005
            ENDIF
            IF (TIME.GT.TIMED) THEN
               I0 = 0.
            ENDIF
            MM = MM + 1
C           IF (NT.GT.NPRINT) THEN
            IF (X.GT.XPRINT) THEN
              XPRINT = X + XINC
              NT = 0
              RATE = 100.*(KSUBP*CONCM*CONCMR)/CONCM0
              RATEV = 100.*(VX-V)/TIMEIC/(VM-VP)
              MM = 0
           WRITE (*,100) TIME,X,RATE,VSUBF,KSUBP,KSUBT
                IF (X.GT.0.995) GO TO 85
         ENDIF
         IF (TIME.LT.TIMETO) GO TO 3
  100    FORMAT (1X,F8.4,3(1X,F7.4),2(1X,e12.3))
  85     RATE = 100.*(KSUBP*CONCM*CONCMR)/CONCM0
         RATEV = 100.*(VX-V)/TIMEIC/(VM-VP)
         WRITE (*,100) TIME, X, RATE,VSUBF, KSUBP,KSUBT


         END


105  0.035  0.50
5.0e6  0.099 12.0  1
0.1060  150
0.93  0.86
0.0005  0.000075
-100  55  30
0.004141  1.0
3000  0.01
1.0
10000
```

Appendix B. Abbreviations

TDP: Transdermal Photopolymerization

PEODM: Poly(ethylene oxide) dimethacrylate

PEG: Poly(ethylene glycol)

HPK: 1-Hydroxycyclohexyl phenyl ketone

GAG: glycosaminoglycans

MTT: 3-(4,5-dimethylthiazol-2-yl)-2,5-diphenyl-2H-tetrazolium bromide

MW: Molecular Weight